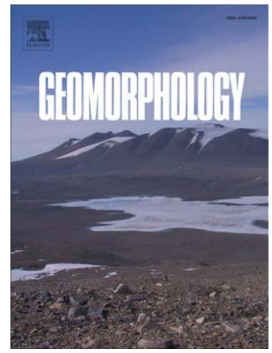

Deep-seated gravitational slope deformation, large-scale rock failure, and active normal faulting along Mt. Morrone (Sulmona basin, Central Italy): Geomorphological and paleoseismological analyses

S. Gori, E. Falcucci, F. Dramis, F. Galadini, P. Galli, B. Giaccio, P. Messina, A. Pizzi, A. Sposato, D. Cosentino

PII: S0169-555X(13)00593-X
DOI: doi: 10.1016/j.geomorph.2013.11.017
Reference: GEOMOR 4568

To appear in: *Geomorphology*

Received date: 30 December 2012
Revised date: 20 November 2013
Accepted date: 24 November 2013

Deep-seated gravitational slope deformation, large-scale rock failure, and active normal faulting along Mt. Morrone (Sulmona basin, Central Italy): geomorphological and paleoseismological analyses.

Gori S.[a,]*, Falcucci E.[a], Dramis F.[b], Galadini F.[a], Galli P.[c], Giaccio B.[d], Messina P.[d], Pizzi A.[e], Sposato A.[d], Cosentino D.[b]

[a] Istituto Nazionale di Geofisica e Vulcanologia (INGV), Italy
[b] Università degli Studi Roma Tre, Roma, Italy
[c] Dipartimento della Protezione Civile Nazionale, Italy
[d] Consiglio Nazionale delle Ricerche, Istituto di Geologia Ambientale e Geoingegneria (CNR-IGAG), Italy
[e] Università "G. d'Annunzio", Chieti, Italy

***Corresponding author.** Tel : +39-339-2602536.

E-mail address: stefano.gori@ingv.it (S. Gori)

Abstract

Active faulting is one of the main factors that induce deep-seated gravitational slope deformations (DGSDs). In this study, we investigate the relationships between the tectonic activity of the NW–SE normal fault system along Mt. Morrone, central Apennines, Italy, and the evolution of the associated *sackung*-type DGSD. The fault system is considered to be the source of M 6.5–7 earthquakes. Our investigations have revealed that the DGSD began to affect the Mt. Morrone SW slope after the Early Pleistocene. This was due to the progressive slope instability arising from the onset of the younger western fault, with the older eastern fault acting as the preferred sliding zone. Paleoseismological investigations based on the excavation of slope deposits across gravitational troughs revealed that the DGSD was also responsible for the displacement of Late Pleistocene–Holocene sediments accumulated in the *sackung* troughs. Moreover, we observed that the investigated DGSD can evolve into large-scale rock slides. Therefore, as well as active normal faulting, the DGSD should be considered as the source of a further geological hazard. Overall, our approach can be successfully applied to other contexts where active normal faults control the inception and evolution of a DGSD.

Keywords: Large-scale slope instability; Active normal faulting; Trenching technique; *Sackung*; Rock avalanche; Sulmona basin; Central Italy.

1. Introduction

Worldwide investigations on mountain slopes have resulted in the identification of geomorphic signatures of large-scale, Deep-seated Gravitational Slope Deformations (DGSDs). These phenomena can be largely divided into three types: *sackung* (originally a German term for sagging, first used by Zischinsky, 1969), lateral spreading, and rock-block slide (e.g., Jahn, 1964; Zischinsky, 1969; Varnes, 1978; Dramis and Sorriso-Valvo, 1994; Dramis et al., 1995; Bisci et al., 1996; Pasuto and Soldati, 1996; Onida, 2001; Soldati, 2004).

Among the factors that induce DGSDs, the available literature has generally assigned a primary role to tectonics (e.g. Gonzalez-Diez et al., 1999; Galadini, 2006; McCalpin, 2009; Audemard et al., 2010). Indeed, active faults make hillslopes unstable by: increasing local relief; juxtaposing/superposing rocks with different mechanic behaviours; producing structural discontinuities such as fault planes, foliations, joints and fractures that can act as sliding surfaces;

and causing ground shaking during the associated seismic events (e.g., Dramis et al., 2002; McCalpin, 2009).

To analyse the role of active tectonics in triggering large-scale gravitational slope movements, the central Apennine chain can be considered as a first-rate case study. This mountain belt has been affected by uplift since the Early Quaternary (D'Agostino et al., 2001 and references therein; Bartolini et al., 2003) as well as by active faulting (Barchi et al., 2000; Galadini and Galli, 2000; Boncio et al., 2004). Many studies have identified DGSDs along the mountain slopes of the central Apennines, and discussed the relationships between the DGSDs and tectonically controlled landscape modification (e.g., Dramis et al., 1987; 2002; Farabollini et al., 1995; Aringoli et al., 1996; Folchi Vici D'Arcevia et al., 1996; Di Luzio et al., 2004; Galadini, 2006; Moro et al., 2012). More recently, studies on large-scale gravitational phenomena have benefited from satellite interferometry techniques (e.g., differential interferometry synthetic aperture radar; Moro et al., 2009) which have allowed the triggering role of earthquakes to be evaluated (Moro et al., 2007, 2011).

The present study deals with the relationships between active normal faulting and the occurrence/evolution of a DGSD through an analysis of the south-western flank of Mt. Morrone, which is affected by an active normal fault system and by large-scale, deep-seated mass-wasting (Ciccacci et al., 1999; Miccadei et al., 2004). Our main goal was to define the kinematic history, style and chronology of the DGSD, with reference to a possible triggering role of normal faulting. We coupled geological/geomorphological field analyses with the application of paleoseismological techniques. Such a method has been used to investigate gravity-driven processes in various areas of the world (e.g., McCalpin and Irvine, 1995; Gutiérrez et al., 2005, 2008, 2010) including the Italian Alps (Forcella et al., 2001) and the Apennines (Moro et al., 2012).

This paper is organised as follows: after the description of the neotectonic framework of the central Apennines and the structural/geomorphic setting of the south-western slope of Mt. Morrone, we present the results of investigations on the DGSD with the data gathered and discussion in terms of structural/geomorphic evolution, chronology, mechanism and style of the DGSD.

2. Geological framework

2.1. Neotectonic setting of the central Apennines

The formation of the Apennine chain is closely related to the westward subduction of the Adriatic lithosphere and its progressive eastward flexural retreat (Patacca and Scandone, 1989). This consists of a fold and thrust belt that progressively migrated eastwards and north-eastwards, which displaced thousands-of-metres-thick Meso-Cenozoic carbonate and siliciclastic sequences (Cosentino et al., 2010 and references therein). The migration of the contractional deformation towards the Adriatic foreland was followed by an extensional tectonic regime that has affected the innermost portions of the chain since the Mio-Pliocene (Cavinato and De Celles, 1999). This new tectonic phase resulted in normal fault systems that dismembered the previously active compressive structures and progressively migrated towards the east and northeast, comparably to the contractional deformation (e.g., Galadini and Messina, 2004; Fubelli et al., 2009). Extensional tectonics proceeded contemporary to the chain uplift, the latter being estimated at about a thousand metres during the whole of the Quaternary (D'Agostino et al., 2001).

In the central Apennines, the activity of the normal fault systems during the Plio-Quaternary resulted in the formation of several half-graben structures that currently match intermontane basins and host continental deposition. These include the Fucino, L'Aquila, Sulmona, Rieti, Leonessa and Norcia basins. Normal and normal-oblique faults generally bound these depressions to the northeast and affect steeply dipping, west- and southwest-facing fault-related mountain slopes that were mainly carved onto the above-mentioned Meso-Cenozoic carbonate bedrock.

Active extension in the central Apennines is supported by: 1) the displacement of Late Pleistocene–Holocene deposits and/or landforms along many of the central Apennine normal faults (e.g., Barchi et al. 2000; Galadini and Galli, 2000; Boncio et al., 2004; Roberts and Michetti, 2004; Galadini et al., 2009; Falcucci et al., 2011); 2) the instrumental seismicity, characterised by earthquakes originating along the northwest-southeast trending normal ruptures (Bagh et al., 2007; Chiarabba et al., 2009; Chiaraluce, 2012); 3) geodetic (GPS) data indicating a 3 mm yr^{-1} extension rate across the belt (D'Agostino et al., 2011; Devoti et al., 2011); and 4) the tectonic stress data derived from borehole breakout measurements (Mariucci et al., 2010 and references therein).

The active normal fault systems in and around the study area (Fig. 1) are generally considered as the surface expression of the seismogenic sources that are potentially responsible for high-magnitude (up to 7) earthquakes (Galadini and Galli, 2000 and references therein; Vannoli et al., 2012 and references therein). The information derived from the available historical seismic catalogues (e.g., Rovida et al., 2011), coupled with geologically and paleoseismologically inferred data (Galli et al., 2008 and references therein), have allowed relating some of the central Italian seismic events to the activation of some westernmost faults. These include the 1349 (Mw = 6.6), 1703 (6.7), 1703 (6.7) and 1915 (7.0) earthquakes. On the other hand, the eastern normal faults that comprise the Assergi-Campo Imperatore, Mt. Vettore, Laga Mts. and Mt. Morrone fault systems have not been activated in historical times (see ACIF, MVF and MMF in Fig. 1, respectively). For this reason, these structures have been defined as silent and are considered as probable seismic gaps (Galadini and Galli, 2000).

2.2. Mt. Morrone south-western slope

Mt. Morrone is an anticline structure that grew due to the activity of a northeast-verging thrust during the Late Messinian to Early Pliocene (Cipollari and Pipponzi, 2003). This thrust involved Meso-Cenozoic limestone and marl pertaining to different paleogeographic domains (i.e., basinal sequences). These are exposed in the northern sector of Mt. Morrone, which transitionally changes to carbonate platform sequences in the southern portion of the relief (Giovannelli, 1992).

Since the Early Pleistocene, the back-limb of the Mt. Morrone anticline has been affected by a ca. 23-km-long, southwest-dipping normal fault system that displaced the carbonate sequences. This gave rise to the Sulmona basin, a half-graben intermontane depression that hosted a continental sedimentary succession through the whole Quaternary (Fig. 2a). Geological field investigations (e.g., Miccadei et al., 1998; Gori et al., 2011, and references therein) have described the Mt. Morrone normal fault system as consisting of two main parallel segments: the western and eastern fault branches. The geomorphic expression of these branches is seen as two up to 100 m high fault scarps affecting the middle-upper sector and the base of the slope, respectively.

This fault system is considered to be presently active, as both fault segments displace Late Pleistocene to Holocene slope and alluvial fan deposits (e.g., Vittori et al., 1995; Miccadei et al., 1998 and references therein; Galadini and Galli, 2000). Recently, geological investigations on the continental sequences that outcrop in the Sulmona basin and along the Mt. Morrone slopes have allowed the updating of the Late Quaternary slip-rate estimates for each fault branch (Gori et al., 2011): 0.4±0.07 mm yr^{-1} for the western splay, and a comparable rate for the eastern splay.

From a seismotectonic point of view, the Mt. Morrone fault system is considered as the surface expression of a seismogenic source that is potentially responsible for M 6.6 to 6.7 earthquakes (Gori et al., 2011). Its last activation probably occurred ca. 1800 years ago, as proposed by Ceccaroni et al. (2009) on the basis of archeoseismological data, which show evidence of an episode of widespread destruction in the Sulmona basin during the 2nd century AD, likely due to a local strong earthquake.

As shown by Gori et al. (2007), the tectonic structure of Mt. Morrone is characterised by a complex Quaternary structural evolution that has strongly conditioned the present geomorphic setting of the southwest-facing slope. In more detail, a progressive basin-wards fault activation probably occurred during the Middle Pleistocene, where the western splay was activated after the eastern splay (Pizzi and Pugliese, 2004; Gori et al. 2007). This structural evolution resulted in an evident staircase slope topography made up of two steeply inclined slope sectors with a wide and almost flat paleo-landsurface between them (Figs. 2a and 3).

The south-western slope of Mt. Morrone is also characterised by widespread, roughly ridge-parallel, troughs, up-hill-facing scarps, and closed depressions (Fig. 2b). These landforms suggest that the slope is affected by a *sackung*-type DGSD. However, besides a geomorphological description of these gravity-related landforms (e.g, Ciccacci et al., 1999; Miccadei et al., 2004), the Mt. Morrone DGSD has never been investigated in detail, in terms of its origin, kinematic history, and Late Quaternary activity.

3. Geomorphologic and structural investigations

3.1. General geomorphic signatures of slope deformation

Aerial photograph analyses and field surveys have allowed us to map in detail the *sackung* landforms along the Mt. Morrone south-western slope. We identified multiple ridge-parallel troughs, closed depressions with uphill- and downhill-facing scarps located at different elevations. There is also as an evident double crest line, marked by a wide ridge-crest ”graben” on top of the relief (Fig. 3). These landforms, mostly detectable at the head of huge unstable rock masses laterally bounded by streams with curvilinear patterns (in plain view), typically display an outward bulging at their toe, resulting in a convex topographic profile.

Our observations indicate that the *sackung* landforms affect the slope sector between the two normal fault branches. In particular, the eastern fault splay coincides with the ridge-crest graben and the uphill side of the main gravitational troughs (Fig. 3, inset). The western fault branch, instead, bounds the sagging rock masses towards the basin (Fig. 3). Moreover, many other minor troughs affect the bulged lower sectors (Fig. 3) where the limestone rocks are pervasively affected by northwest–southeast trending and mainly southwest-dipping steep shear planes, joints, cleavage planes and fractures. These observations suggest that some of the mentioned fault-related features accommodate the gravitational deformation. As described in the following paragraph, two of these secondary gravitational troughs were selected for investigations by using paleoseismological methods.

In some places, scarps related to the western fault splay appear to be displaced by DGSD movement. This is evident in some sectors at the base of the slope, for instance, at Roccacasale (Fig. 4a), downslope of the Colle della Paglia gravitational trough. Indeed, the fault plane and the related scarp (10 to 15 m high) appear to be horizontally shifted towards the Sulmona basin with respect to the fault-trace trend. Instead, about a dozen metres uphill we have recognized a continuous ribbon-like fault scarplet aligned with the northern and southern prolongations of the fault branch. As limestone crops out both in the fault footwall and the hanging wall (Fig. 4b), this feature cannot be related to non-tectonic processes, such as selective erosion or landslides that affect the hanging wall block. Furthermore, slope debris, probably Late Pleistocene to Holocene in age (Gori et al., 2011), has been dragged in some places along this fault (Fig. 4c). On the other hand, the westernmost fault scarp, probably displaced by the gravitational deformation, is strongly affected by karstic erosion. Moreover, the base of the scarp is largely covered with scree thus suggesting the absence of tectonic displacement. These observations indicate the formation of a brand-new, uphill rupture that might represent the current surface expression of the tectonic structure. However, a certain amount of coseismic slip along the older fault planes during an activation event of the Mt. Morrone normal fault cannot be completely ruled out.

3.2. The Le Pietre-Pianezza rock slide

In the Le Pietre-Pianezza locality, a few dozen metres north of Roccacasale, a huge rock mass slid for some hundred metres towards the basin (Fig. 4a). The rock slide shows an outwards convex profile and a topmost portion characterised by an almost flat sector, where slope deposits can accumulate. The rock slide scarp is visible upslope of the accumulation body and it roughly coincides with the northern prolongation of the above-described ribbon-like scarplet in the Roccacasale area. Moreover, a series of up to 10–15 m high parallel remnants of fault scarps are seen along the slid block (Fig. 5a–c), which displays a curved trend in plan view. These observations suggest that: 1) the western fault splay periodically cut the rock masses, forming a fault-related scarp; 2) this scarp was subsequently displaced and shifted towards the basin by the movement of the rock slide; and 3) the fault subsequently cut the sliding masses again, forming a new scarp. The repetition of this sequence over time has led to the formation of a series of new fault scarps that get progressively younger upslope (Fig. 5d). Such gravity/tectonics-coupled processes are also suggested by the intense karstic weathering of the lowermost fault scarps observed along the rock slide accumulation body. This testifies to the lack of rejuvenation of the fault-related landforms, as they might not be linked anymore to the fault at depth (as indicate before, a certain amount of coseismic slip along the older fault planes cannot be completely ruled out). Conversely, the continuous ribbon-like fault scarplet described might represent the presently active surface expression of the fault segment. We can hypothesize that the local slope instability that led to the rock sliding was induced by an increase of local relief due to the activity of the fault segment and the progressive deepening of the Sagittario River that, in this sector, flows along the foot of the rock slide.

3.3. The Pacentro paleo-landslide

In the locality of *Vallone di Mileto* (Figs. 3 and 6a), in the southernmost sector of the Mt. Morrone south-western slope, there is a landslide scarp some hundred metres wide and high, running between the tips of the two fault branches (Fig. 6b,c). The scarp is superimposed onto the above-described double-crested ridge (Fig. 6b–e). A huge fan-shaped landslide body of carbonate rock with a volume of thousands of m^3 is located at the base of the slope above which the Pacentro settlement is partly located. Miccadei et al. (1998) inferred that this landslide occurred in the Early Pleistocene (the “Pacentro paleo-landslide”). This chronology is confirmed by the presence of Middle Pleistocene alluvial fan sediments (Giaccio et al., 2009; Gori et al., 2011), both within the main landslide scarp at the footwall of the western fault branch, and on the landslide debris at the hanging wall of the fault branch (Fig. 6b). The chronological reference of the alluvial fan sediments is derived from their relationships with chronologically constrained lacustrine and fluvial deposits of the Sulmona basin (Galli et al., 2010; Falcucci, 2011). This defines a *terminus ante quem* for the landsliding event.

Along with the geomorphic relationships, the correlation between the Mt. Mileto scarp and the Pacentro paleo-landslide is also supported by the landslide accumulation made of fragments of the Jurassic–Cretaceous limestone that outcrops along the Mt. Morrone southern sector (Vezzani and Ghisetti, 1998). In addition, the volume of the Pacentro paleo-landslide appears to be consistent with the scarp size, although this is a rough estimate because the landform has been deeply reshaped by several streams cutting across the mountain flank. As the landslide has a single top surface and there is no paleosol within the accumulated debris, we can hypothesise that the Pacentro paleo-landslide resulted from a single, sudden, catastrophic movement.

4. Paleoseismological techniques applied to deep-seated gravitational slope deformations

We made four trenches for paleoseismological investigations across two gravitational troughs along the slopes of Mt. Orsa and Colle della Paglia (Fig. 3). The analysis of the trench walls and the infilling sequences provided information useful for defining the sub-surface geometry of the troughs, their chronology, current activity and style of deformation.

The sedimentary sequences exposed by the trenches mainly consisted of silty and coarse-grained slope deposits that were derived from the erosion of the carbonate bedrock and/or the re-deposition of Quaternary sediments. Moreover, paleosols were detected at different stratigraphic levels. Radiocarbon dating of the paleosols and charcoals in the deposits has provided chronological constraints for the slope deformation history (Table 1).

4.1. Mt. Orsa site

4.1.1. Morphostructural setting

The Mt. Orsa gravitational trough is about 1 km long and 150 m wide and is located at elevations between 620 and 680 m a.s.l. (Fig. 7a,b). This *sackung* landform is bounded by two scarps that are carved onto the carbonate bedrock: a downhill-facing scarp that bounds the uphill side of the trough, and an uphill-facing steeper scarp that bounds the downhill flank (Fig. 7c).

Our field surveys revealed the displacement of slope-derived breccias due to the spreading of the gravitational depression. These sediments make part of a complex of slope/alluvial deposits widespread in the central Apennines ("*Brecce Mortadella*") and commonly referred to the Early Pleistocene (e.g., D'Agostino et al., 1997; Miccadei et al., 1998; Bosi et al., 2003; Gori et al., 2007). The Mt. Orsa breccias (inset of Fig. 7b) were emplaced on the paleo-landsurface between the two fault splays (see Section 2.1) before the formation of the western fault branch (Gori et al., 2007). The uphill side breccias gently dip towards the trough (Fig. 7d) while those outcropping on the downhill side are deformed and tilted, likely due to trough spreading (Fig. 7d, inset). Hence, the gravitational depression of Mt. Orsa formed after the deposition of the Early Pleistocene breccias.

4.1.2. Sedimentology and chronology of deposits of trenches

We dug two trenches each of which was 9 m long, 2.5 m deep, and 2.5 m wide. One was across the downhill-facing scarp (eastern trench), and the other was across the uphill-facing scarp (western trench). These uncovered a succession of slope sediments in contact with the carbonate bedrock along the scarps of the gravitational trough (Fig. 8a,b).

At the bottom of the trenches, we observed the carbonate bedrock of the uphill slope dragged against that of the downhill side through a few-cm-thick fracture that filled with colluvial deposits (Fig. 8c,d). A basic description of the deposits exposed by both trenches is provided here.

- Unit Or1: Colluvial deposit made up of heterometric carbonate sub-angular gravels with a silty-sandy brown matrix that contains indeterminable pottery fragments. At the base of the unit, a stone line with pebbles 1 to 4 cm in length marks an erosional surface that truncates Unit Or2.
- Unit Or2: Ochre-brown sand and clay that contain charcoal fragments and sparse sub-angular carbonate pebbles 1 to 5 cm in length.

- Unit Or3: Ochre sandy-clayey colluvial deposits containing volcanic tephra (mainly composed of black mica and pyroxenes) the abundance of which increases with depth. We obtained radiocarbon dating of both bulk paleosol and charcoals lying over this unit, 4240–3920 BP (cal. 2σ) and 2340-2130 BP (cal. 2σ), respectively. Moreover, a charcoal fragment sampled at the bottom of the unit gave an age of 41,390-40,290 BP (cal. 2σ).
- Unit Or4: Carbonate bedrock that crops out along the trough scarps and at the bottom of the depression.

The dating of Unit Or3 indicates that the trough probably formed around 40 kyrs BP, with the lowermost sample collected only about 30 cm above the carbonate bedrock.

4.1.3. Slope deformation

The trough opening resulted in gravitational instability of a downhill portion of the depression. The limestone was clearly shifted towards the trough, overthrusting the slope deposits (Fig. 8a,c). The scarp of this small rock slide is detectable along the uphill-facing scarp (Fig. 8e), with a sliding surface dipping towards the trough bottom (Fig. 8c,f).

4.2. Colle della Paglia site

4.2.1. Morpho-structural setting

The Colle della Paglia gravitational trough (800 m a.s.l.) is 1-km long and 150-m wide (Fig. 9b). The depression is bounded by a downhill-facing scarp to the south-west, and a steeper uphill-facing scarp to the north-east. Two trenches (eastern and western), about 9 m long, 2.5 m deep and 2.5 m wide each, were dug in the northernmost part of the depression, across the downhill-facing and uphill-facing scarps (Fig. 9c).

4.2.2. Sedimentology and chronology of deposits of the western and eastern trenches

The two trenches exposed different successions of slope deposits (Fig. 10a–d) infilling the depression. The units found in the western trench are listed below (CpW1–13).

- Unit CpW1. Brown sandy silt containing sparse angular-to-subangular carbonate pebbles. A paleosol dated at 2950–2760 BP (cal. 2σ) separates this unit from the underlying one.
- Units CpW2–4. Yellowish-reddish clayey-silty colluvial deposits, probably derived from the erosion and re-sedimentation of organic-rich sediments and/or pedogenetic horizons. Units CpW2, CpW3, and CpW4 are separated by two paleosols dated at 12,610–11,860 BP (cal 2σ) and 21,560–21,320 BP (cal. 2σ). Towards the downhill side of the trough, Units CpW3 and CpW4 grade laterally into the deposits of Unit CpW5.
- Units CpW5 to CpW11. Succession of slope deposits mainly made up of angular to subangular carbonate pebbles, with a mainly open-work and clast-supported texture, which were distinguished on the basis of different grain sizes, matrix colours and textures (i.e., matrix-supported *vs* clast-supported). Their general sedimentological and stratigraphic features, and their relationships with the upper chronologically constrained deposits suggest that they formed due to periglacial slope processes in the Last Glacial period (Castiglioni et al., 1979; Coltorti and Dramis, 1988).
- Unit CpW12. Greyish-brownish sandy-silty paleosol that was radiocarbon dated at 33,451–32,851 BP (cal. 2σ).
- Unit CpW13. Limestone bedrock.

Five units (CpE1–5) were identified from the eastern trench:

- Unit CpE1. Brown sandy silt containing sparse angular-to-subangular carbonate pebbles.
- Unit CpE2. Brown silty-sandy colluvial deposit. An erosional surface was observed at the boundary of Units CpE1 and CpE2.
- Unit CpE3. Ochre silty-sandy colluvium with grey paleosol on top.

- Unit CpE4. Reddish clayey-silty sediment. An erosional surface, marked by a line carbonate pebbles, separated this unit from the above unit.
- Unit CpE5. Carbonate bedrock (layer attitude N290°, 43°).

4.2.3. Slope deformation

The radiocarbon dating of Unit CpW12 indicates that the formation of the Colle della Paglia gravitational-trough occurred before ca. 33 kyrs BP. Similar to the Mt. Orsa trough, a small rock slide driven by a shear surface had displaced part of the uphill-facing scarp. This mass movement may have been induced by the gravitational instability of the uphill-facing scarp due to the progressive opening of the trough. As the rock slide overlaid Unit CpW12, we can hypothesise that the trough opening continued after ca. 33 kyrs BP.

Moreover, Units CpW3–5 have been displaced along several trough-parallel shear planes that displayed normal kinematics (Fig. 10e,f). These structural features were sealed by the paleosol that developed on Unit CpW3. The radiometric ages for these units written in Section 4.2.2, displaced by the shear planes, indicate that they activated between 21,560–21,320 BP (cal. 2σ) and 12,610–11,860 BP (cal 2σ). From a kinematic point of view, these structural features might represent evidence of an abrupt settlement of the Colle della Paglia depression that was driven by a rapid movement of the underlying rock mass.

5. Discussion

5.1. Structural evolution of the slope and deep-seated gravitational deformation

The analyses carried out on the Mt. Morrone south-western slope suggest a direct relationship among the activity of the normal fault system, its structural evolution and the occurrence of slope sagging. *Sackung* features are located only in the sector between the two normal fault segments. The eastern fault segment matches with the upslope side of the main gravity-driven troughs, while the western segment bounds the toe of the unstable rock masses. This inferred geomorphic development illustrated in Fig. 11 suggests that the main factors that conditioned the onset and evolution of the DGSD were the increase of local relief and the over-steepening of slopes caused by the activity of the western fault branch. The eastern branch, instead, is used in its surficial portions as the deep-seated slip surface of the mass-wasting..

In terms of the structural relationships between the fault splays and the *sackung*-related features, it is worth noting that the counter-slope scarp of the main gravitational trough might have originated as an antithetic fault of the eastern fault splay. Nevertheless, at present, no fault planes are exposed along the scarp, the landform has an arcuate and complex shape in plan view with a rather discontinuous trace, and the trough width is much smaller than would be expected if this were a tectonic graben between the eastern fault splay and an antithetic fault.

The recent scarp rejuvenation and the progressive spreading of the trough were probably led by gravity-driven slope processes (see McCalpin, 2009 for the criteria to distinguish *sackung*-related features from tectonic ones). In a general perspective, this observation implies that in cases where active faults traces and large-scale mass wasting scarps coincide, estimations of earthquakes magnitudes based on surface-fault offsets (Wells and Coppersmith, 1994) may be tainted by gravitational components of displacement. Also, the counter-slope scarp of the main troughs may be used at present for accommodating the gravitational deformation at its shallower portion.

As a consequence of the activity of the normal fault branches, the displacement of the back-limb of the Mt. Morrone anticline has exposed anti-slope dipping carbonate strata which are not favourable to landsliding. Nevertheless, normal faulting has also led to the formation of dip-slope structural features in the rock masses, i.e. fault planes, shear planes, and extensional fractures that weaken the rock mass and that can be used as sliding planes (Fig. 11). The depicted framework testifies to a cause–effect relationship between normal faulting and the occurrence of the DGSD.

5.2. Chronology of deformation

According to Gori et al. (2007), the western fault splay was formed after the eastern branch, in a moment subsequent to the Early Pleistocene (Fig. 11). The same chronological constraint can also be inferred for the activation of the DGSD. This agrees with the observed displacement of the Early Pleistocene breccias, which were deposited along the slope before the activation of the western fault branch (see Section 4.1).

For the recent kinematic history of the Mt. Morrone DGSD, useful information has been derived from the stratigraphic sequences uncovered by our Mt. Orsa and Colle della Paglia excavations coupled with the radiocarbon dates. Our data indicate that the Mt. Orsa trough formed during the Late Pleistocene, probably around 40 kyrs BP, i.e. the age of the charcoal found in Unit Or3 as the charcoal was collected almost at the base of the sedimentary succession. For the Colle della Paglia depression, we can only state that the trough opening began at some time before 33 kyrs BP.

Furthermore, the continuous accumulation of slope debris within the depressions during the Late Pleistocene–Holocene and the shear planes that we detected at the Colle della Paglia trough site (Fig. 10b) suggest that the opening of both the gravitational troughs has persisted over the last few thousands of years. Therefore, the Mt. Morrone DGSD can be regarded as presently active.

5.3. Mechanism and style of deformation

As shown in Fig. 8c, the excavations at the Mt. Orsa site suggested that the depression originated from progressive opening of a fracture system that affected the carbonate bedrock, due to the downslope movements of the unstable rock masses. A similar mechanism probably formed the Colle della Paglia trough as well.

In terms of the regime of deformation, the available literature indicates that *sackung*-type features generally evolve with long-term creep movement (Bisci et al., 1996), even if episodic accelerations of the deformation can occur (McCalpin, 2009 and references therein). Thus, creep probably represents the predominant style of deformation of the investigated DGSD. Nevertheless, the shear planes detected within the Colle della Paglia trough, which were responsible for the displacement of Units CpW3, CpW4 and CpW5, can be considered as brittle deformation structures, thus suggesting the occurrence of abrupt gravitational displacement (McCalpin, 2009). Taking into account the chronological constraints for the displaced units, this deformation event probably occurred between 21 and12 kyrs BP.

In terms of the cause of this event, it must be taken into account that re-activation of the DGSD has been observed during strong earthquakes in Italy (i.e. the 1997 Umbria-Marche earthquake sequence and the 2009 L'Aquila earthquake; Moro et al., 2007, 2011, respectively). Hence, if we consider the seismotectonic framework of Mt. Morrone and more in general, of the central Apennines, we can hypothesise that the displacement event at Colle della Paglia was triggered by a strong earthquake that occurred in the surrounding regions or even along the Mt. Morrone normal fault system. It is worth noting that coseismic input has been invoked in several studies (e.g., McCalpin, 2009 and references therein), where dynamic loading produced by seismic events is indeed considered as a primary factor influencing the genesis and evolution of slope sagging features. In addition, other paleoseismological studies in the central Apennines have revealed the probable triggering of large-scale mass wasting by the coseismic activation of nearby active faults (Moro et al., 2012).

On the other hand, our paleoseismological analyses did not provide evidence for the activation of gravity-driven displacement due either to the second century AD earthquake along the Mt. Morrone fault system (Ceccaroni et al., 2009), or to the other known high-magnitude historical seismic events in 1349, 1456, 1706, and 1933. This observation would therefore suggest that in spite of the strong ground motion produced by these large-magnitude earthquakes, these events did not induce deformation ”large” enough to be detectable with standard paleoseismological techniques, or to be univocally interpretable as seismically induced sedimentary features (i.e., colluvial wedges in McCalpin, 2009). Therefore, in agreement with McCalpin (2009), the deformation history of *sackung* features cannot be used, if taken alone, as paleoseismological indicators.

5.4. DGSD evolution in relation to surface faulting

Our data indicate that the investigated *sackung*-type deformation can evolve into a large-scale gravitational phenomenon, with either a low moving rate or a sudden rapid motion. In the former case, the shape of the abandoned fault scarps along the Le Pietre-Pianezza rock slide suggests the progressive movement of the rock mass towards the Sulmona Basin. The curved trace of the scarps along the rock slide indicates that the landforms have been deformed with slow continuous displacement. Therefore, the progressive movements of the rock slide prevented the fault there from rupturing and led to the formation of a new fault scarp slightly upslope. Papanikolaou et al. (2005) considered the lowermost fault scarp along the Le Pietre-Pianezza rock slide as the result of repeated surface faulting episodes of the western fault branch, and estimated a post-LGM fault slip rate of 0.84±0.17 mm yr^{-1} from the scarp height. Our observations suggest, however, that this scarp does not represent the surface expression of an active fault, as it was probably displaced by the Le Pietre-Pianezza rock slide. Therefore, the slip rate estimated at this site by Papanikolaou et al. (2005) should be taken at least with some caution, as this fault scarp might be not linked to the primary fault anymore. In general, dating of active faulting or paleoseismological events based on geomorphological analyses (e.g., Papanikolaou et al., 2005) or exposure dating (e.g., Schlagenhauf et al., 2011) must take into account the possible interaction between mass wasting and faulting, as the fault planes may be exposed by other non-tectonic processes.

Our observations yield implications on hazards of surface fault rupture. Boncio et al. (2012) proposed a fault setback, i.e., the distance from the active fault trace within which critical facilities and structures designed for human occupancy cannot be built, for the Mt. Morrone western fault splay at the southern tip of the Le Pietre-Pianezza rock slide. The defined setback includes the fault scarps that may have been displaced by the rock slide, while it only partially encloses the fault scarplet that probably represents the current surface expression of the active fault.

In contrast to the Le Pietre-Pianezza rock slide, the Pacentro paleo-landslide testifies to a rapid and catastrophic evolution of a *sackung*-related landform. Indeed, as described above, the main scarp of the landslide is carved into the double-crested sector of Mt. Morrone, and the rock slope failure displaced rock masses that were already affected by sagging. Moreover, the proximity between the described rock avalanche and the Mt. Morrone normal fault system, or other nearby Quaternary fault systems, allows us to hypothesise that the landslide was triggered by an ancient, large-magnitude seismic event that produced strong and long-lasting shaking originated from either the Mt. Morrone fault or a nearby tectonic structure. This inference agrees with the relationships among landslides, fault-rupture zones and earthquake magnitudes proposed by Keefer (1984).

6. Concluding remarks

In this study, we show the results of geological/geomorphological/paleoseismological investigations on the south-western slope of Mt. Morrone, Italy. The slope has been affected by an active normal fault system with two NW–SE-trending and SW-dipping parallel branches, and by a DGSD specifically related to sagging. The goal of our analyses was to define the relationships between the onset and evolution of the DGSD and the Quaternary activity of the extensional tectonic structure. Furthermore, to define the activity of the DGSD, we applied paleoseimological investigations by digging trenches across some landforms along the slope.

Our data have revealed that the DGSD initiated after the Early Pleistocene, following the activation of the western normal fault branch. The activity of this fault branch resulted in increased local relief, while the eastern fault segment acted as a sliding plane in its surficial portion. Moreover, the activity of both the fault strands resulted in the formation of structural features and discontinuities that weakened the rock mass and provided preferential sliding zones, predisposing the slope to sagging.

The excavations across the *sackung*-related Mt. Orsa and Colle della Paglia troughs indicate that these features formed from the progressive spreading of fractures in the rock mass, at around 40 kyrs BP and before about 33 kyrs BP, respectively. The shear planes in the sedimentary units that were trapped within the Colle della Paglia trough and dated between about 21 and 12 kyrs BP imply the mechanics of the gravitational deformation: although a *sackung* is generally considered to evolve by creep (McCalpin, 2009 and references therein), the shear planes of the Mt. Morrone DGSD represent brittle deformation structures that indicate an event of rapid gravitational collapse. The proximity of the Colle della Paglia trough to the Mt. Morrone normal fault system suggests that this event was triggered by a tectonic activation episode. Furthermore, our observations suggest that the DGSDs can evolve into large-scale gravity-related phenomena characterised either by continuous, low rate movements, as for the Le Pietre-Pianezza rock slide near Roccacasale, and/or by a rapid and even catastrophic collapse, as testified by the Pacentro paleo-landslide.

Our study has also highlighted that investigations on active faults should consider the effect of gravity-driven phenomena because of two reasons:

1) Large-scale mass-wasting can superpose onto tectonic displacements, as in the case of the Mt. Morrone eastern fault branch. This may lead to an incorrect estimation of earthquake magnitudes based on surface-fault offsets; and

2) The occurrence of DGSDs makes the mapping of active faults more difficult due to the gravity-driven displacements of fault scarps.

Acknowledgement

We are grateful to Dr. Franck A. Audemard, Dr. Mauro Soldati and Dr. Tomás Pánek whose comments and suggestions allowed us to improve this paper. We warmly thank the Editor Dr. Takashi Oguchi for the final revision of the manuscript. We also thank Dr. Marco Moro, Dr. Michele Saroli, Dr. Giandomenico Fubelli and Augusto Cittadini for the useful discussion on DGSDs and paleoseismological techniques, and for their help in the fieldwork. Part of this work has been carried out within the partnership between Istituto Nazionale di Geofisica e Vulcanologia and Dipartimento della Protezione Civile (2004–2006 and 2007–2009).

References

Aringoli, D., Gentili, B., Pambianchi, G., 1996. The role of recent tectonics in controlling the deep-seated gravitational deformation of Mount Frascare (Central Apennines). Geogr. Fis. Din. Quat. 19, 281–286.

Audemard, F.A., Beck, C., Carrillo, E., 2010. Deep-seated gravitational slope deformations along the active Boconó Fault in the central portion of the Mérida Andes, western Venezuela. Geomorphology 124, 164-177.

Bagh, S., Chiaraluce, L., De Gori, P., Moretti, M., Govoni, A., Chiarabba, C., Di Bartolomeo, P., Romanelli, M., 2007. Background seismicity in the Central Apennines of Italy: the Abruzzo region case study. Tectonophysics 444, 80–92.

Barchi, M., Galadini, F., Lavecchia, G., Messina, P., Michetti, A.M., Peruzza, L., Pizzi, A., Tondi, E., Vittori, E. (Eds.) 2000. Sintesi delle Conoscenze sulle Faglie Attive in Italia Centrale: Parametrizzazione ai Fini della Caratterizzazione della Pericolosita` Sismica. CNR-Gruppo Nazionale per la Difesa dai Terremoti, Roma, 2000, 62 pp..

Bartolini, C., D'Agostino, N., Dramis, F., 2003. Topography, exhumation, and drainage network evolution of the Apennines. Episodes 23, 212-217.

Bisci, C., Dramis, F., Sorriso-Valvo, M., 1996. Sackung (rock flow/sagging). In: Dikau, R., Brunsden, D., Schrott, L., Ibsen, M.-L. (Eds.), Landslide Recognition: Identification, Movement and Causes. J. Wiley & Sons, Chichester, pp.150-160.

Boncio, P., Lavecchia, G., Pace, B., 2004. Defining a model of 3D seismogenic sources for seismic hazard assessment applications: the case of central Apennines (Italy). J. Seismol. 8, 407-425.

Boncio, P., Galli, P., Naso, G., Pizzi, A., 2012. Zoning surface rupture hazard along normal faults: insight from the 2009 Mw 6.3 L'Aquila, central Italy, earthquake and other global earthquakes. Bull. Seismol. Soc. Am. 102, 918‒935.

Bosi, C., Galadini, F., Giaccio, B., Messina, P., Sposato, A., 2003. Plio-Quaternary continental deposits in the Latium-Abruzzi Apennines: the correlation of geological events across different intermontane basins. I1 Quaternario 16(l bis), 55-76.

Castiglioni, G.B., Girardi, A., Sauro, U., Tessari, F., 1979. Grèzes litées e falde detritiche stratificate di origine crionivale. Geogr. Fis. Din. Quat. 2, 64-82.

Cavinato, G.P., De Celles, P.G., 1999. Extensional basins in the tectonically bimodal Central Apennines fold–thrust belt, Italy: response to corner flow above a subducting slab in retrograde motion. Geology 27, 955-958.

Ceccaroni, E., Ameri, G., Gomez Capera, A.A., Galadini, F., 2009. The 2nd century AD earthquake in central Italy: archeoseismological data and seismological implications. Nat. Hazards 50, 335-359.

Chiaraluce, L., 2012. Unraveling the complexity of Apenninic extension fault system: A review of the 2009 L'Aquila earthquake (Central Apennines, Italy). J. Struct. Geol. 42, 2-18.

Chiarabba, C., Amato, A., Anselmi, M., Baccheschi, P., Bianchi, I., Cattaneo, M., Cecere, G., Chiaraluce, L., Ciaccio, M.G., De Gori, P., De Luca, G., Di Bona, M., Di Stefano, R., Faenza, L., Govoni, A., Improta, L., Lucente, F.P., Marchetti, A., Margheriti, L., Mele, F., Michelini, A., Monachesi, G., Moretti, M., Pastori, M., Piana Agostinetti, N., Piccinini, D., Roselli, P., Seccia, D., Valoroso, L., 2009. The 2009 L'Aquila (central Italy) MW6.3 earthquake: main shock and aftershocks. Geophys. Res. Lett. 36, L18308, doi:10.1029/2009GL039627.

Ciccacci, S., D'Alessandro, L., Dramis, F., Miccadei, E., 1999. Geomorphologic evolution and neotectonics of the Sulmona intramontane basin (Abruzzi Apennines, central Italy). Z. Geomorph. NF 118, 27-40.

Cipollari, P., Pipponzi, G., 2003. Le "Calciruditi di Calaturo" (Montagna del Morrone): un deposito tardo-orogenico della fine del Pliocene inferiore. Studi Geologici Camerti, Numero Speciale, 1/2003, 73-83.

Coltorti, M, Dramis, F., 1988. The significance of stratified slope-waste deposits in the Quaternary of Umbria-Marche Apennines, Central Italy. Z. Geomorph NF 71 (Suppl. Bd), 59-70.

Cosentino, D., Cipollari, P. Marsili, P., Scrocca, D., 2010. Geology of the central Apennines: a regional review. In: Beltrando, M., Peccerillo, A., Mattei, M., Conticelli, S., Doglioni, C. (Eds.), The Geology of Italy. Journal ot the Virtual Exploree 36, paper 11.

D'Agostino, N., Jackson, J.A., Dramis, F., Funiciello, R., 2001. Interactions between mantle upwelling, drainage evolution and active normal faulting: an example from the central Appennines (Italy). Geophys. J. Int. 147, 475-479.

D'Agostino, N., Mantenuto, S., D'Anastasio, E., Giuliani, R., Mattone, M., Calcaterra, S., Gambino, P., Bonci, L., 2011. Evidence for localized active extension in the central Apennines (Italy) from global positioning system observations. Geology 39, 291-294.

D'Agostino, N., Speranza, F., Funiciello, R., 1997. Le Brecce Mortadella dell'Appennino Centrale: primi risultati di stratigrafia magnetica. Il Quaternario 10, 385-388.

Devoti, R., Esposito, A., Pietrantonio, G., Pisani, A.R., Riguzzi, F., 2011. Evidence of large scale deformation patterns from GPS data in the Italian subduction boundary. Earth Planet. Sci. Lett. 311, 230-241.

Di Luzio, E., Saroli,M., Esposito, C., Bianchi-Fasani,G., Cavinato, G.P., Scarascia-Mugnozza, G., 2004. Influence of structural framework on mountain slope deformation in the Maiella anticline (central Apennines, Italy). Geomorphology 60, 417-432.

Dramis, F., Sorriso-Valvo, M., 1994. Deep-seated gravitational slope deformation, related landslides and tectonics. Eng. Geol. 38, 231-243.

Dramis, F., Gentili, B., Pambianchi, G., 1987. Deformazioni gravitative profonde nell'area di Monte Gorzano (Monti della Laga, Appennino Centrale). Boll. Soc. Geol. It. 106, 265-271.

Dramis, F., Farabollini, P., Gentili, B., Pambianchi, G., 1995. Neotectonics and large-scale gravitational phenomena in the Umbria-Marche Apennines, Italy. In: Slaymaker, O. (Ed.) Steepland Geomorphology. J. Wiley & Sons, Chichester, pp. 199-217.

Dramis, F., Farabollini, P., Gentili, B., Pambianchi, G., 2002. Neotectonics and large-scale gravitational phenomena in the Umbria–Marche Apennines, Italy. In: Comerci, V., D'Agostino, N., Fubelli, G., Molin, P., Piacentini, T. (Eds.), Seismically Induced Ground Ruptures and Large Scale Mass Movements, Field Excursion and Meeting, Atti APAT 4/2002, vol. 21–27, pp. 17-30.

Falcucci, E., 2011. Evoluzione geomorfologica tardo-quaternaria della media valle dell'Aterno, Appennino Abruzzese. Ph.D. Thesis, "La Sapienza" Università di Roma, Italy.

Falcucci, E., Gori, S., Moro, M., Pisani, A.R., Melini, D., Galadini, F., Fredi, P., 2011. The 2009 L'Aquila earthquake (Italy): what next in the region? Hints from stress diffusion analysis and normal fault activity. Earth Planet. Sci. Lett. 305, 350-358.

Farabollini, P., Folchi Vici D'Arcevia, C., Gentili, B., Luzi, L., Pambianchi, G., Viglioni F., 1995. La morfogenesi gravitativi nelle formazioni litoidi dell'Appennino centrale. Mem. Soc. Geol. It. 50, 123-136.

Folchi Vici D'Arcevia, C.S., Gentili, B., Luzi, L., Pambianchi, G., Viglione, F., 1996. Deep-seated gravitational slope deformation in the central-southern Umbro–Marchean Apennines: morphometric and macrostructural analyses. Geogr. Fis. Din. Quat. 19, 335-341.

Forcella, F., Tibaldi, A., Onida, M., Galadini, F., 2001. Tecniche paleosismologiche per lo studio di deformazioni gravitative profonde di versante in ambiente alpino: esempi nella valle del Foscagno e al passo del Mortirolo (Alpi Centrali, Italia). In: Pasquarè, G. (Ed.), Tettonica Recente e Instabilità di Versante nelle Alpi Centrali. CNR, Istituto per la Dinamica dei Processi Ambientali, Milano, Italy, pp. 35-74.

Fubelli, G., Gori, S., Falcucci, E., Galadini, F., Messina, P., 2009. Geomorphic signatures of recent normal fault activity *versus* geological evidence of inactivity: case studies from the central Apennines (Italy). Tectonophysics 476, 252-268.

Galadini, F., 2006. Quaternary tectonics and large-scale gravitational deformations with evidence of rock-slide displacements in the Central Apennines (central Italy). Geomorphology 82, 201-228.

Galadini, F., Galli, P., 2000. Active tectonics in the central Apennines (Italy)—input data for seismic hazard assessment. Nat. Hazards 22, 225-270.

Galadini, F., Messina, P., 2004. Early–Middle Pleistocene eastward migration of the Abruzzi Apennine (central Italy) extensional domain. J. Geodyn. 37, 57-81.

Galadini, F., Pantosti, D., Boncio, P., Galli, P., Messina, P., Montone, P., Pizzi, A., Salvi, S., 2009. Il terremoto del 6 Aprile e le conoscenze sulle faglie attive dell'Appennino centrale. In: L'Aquila, 6 Aprile 2009, ore 3.32. Progettazione Sismica 3, 37-48.

Galli, P., Galadini, F., Pantosti, D., 2008. Twenty years of paleoseismology in Italy. Earth Sci. Rev. 88, 89-117.

Galli, P., Giaccio, B., Messina P., 2010. The 2009 central Italy earthquake seen through 0.5 Myr-long tectonic history of the L'Aquila faults system. Quat. Sci. Rev. 29, 3768-3789.

Giaccio, B., Messina, P., Sposato, A., Voltaggio, M., Zanchetta, G., Galadini, F., Gori, S., Santacroce, R., 2009. Tephra layers from Holocene lake sediments of the Sulmona Basin, central

Italy: implications for volcanic activity in Peninsular Italy and tephrostratigraphy in the central Mediterranean area. Quat. Sci. Rev. 28, 2710-2733.

Giovannelli, A., 1992. Le unità carbonatiche circostanti la pianura di Sulmona (AQ). Stratigrafia, analisi di facies e paleogeografia. Ph.D. Thesis, Università degli Studi di Roma "La Sapienza", Italy.

Gonzalez-Dıez, A., Remondo, J., Diaz de Teran, J.R., Cendrero, A., 1999. A methodological approach for the analysis of the temporal occurrence and triggering factors of landslides. Geomorphology 30, 95-113.

Gori, S., Dramis, F., Galadini, F., Messina, P., 2007. The use of geomorphological markers in the footwall of active faults for kinematic evaluation: examples from the central Apennines. Boll. Soc. Geol. Ital. 126, 365-374.

Gori, S., Giaccio, B., Galadini, F., Falcucci, E., Messina, P., Sposato, A., Dramis, F., 2011. Active normal faulting along the Mt. Morrone south-western slopes (central Apennines, Italy). Int. J. Earth Sci. (Geologische Rundschau) 100, 157-171.

Gutiérrez, F., Acosta, E., Rìos, S., Guerrero, J., Lucha, P., 2005. Geomorphology and geochronology of sackung features (uphill-facing scarps) in the Central Spanish Pyrenees. Geomorphology 69, 298-314.

Gutiérrez, F., Ortuño, M., Lucha, P., Guerrero, J., Acosta, E., Coratza, P., Piacentini, D., Soldati, M., 2008. Late Quaternary episodic displacement on a sackung scarp in the central Spanish Pyrenees. Secondary paleoseismic evidence? Geodin. Acta 21, 187-202.

Gutiérrez, F., Lucha, P., Galve J.P. 2010. Reconstructing the geochronological evolution of large landslides by means of the trenching technique in the Yesa Reservoir (Spanish Pyrenees). Geomorphology 124, 124-136.

Jahn, A., 1964. Slopes morphological features resulting from gravitation. Z. Geomorph. N.F. Suppl.-Band 5, 59-72.

Keefer, D.K., 1984. Landslides caused by earthquakes. Geol. Soc. Am. Bull. 95, 406-421.

Mariucci M.T., Montone P., Pierdominici S., 2010. Present-day stress in the surroundings of 2009 L'Aquila seismic sequence (Italy). Geophys. J. Int. 182, 1096-1102.

McCalpin, J., 2009. Paleoseismology, 2nd edition. Academic Press, Amsterdam, 848 pp.

McCalpin, J.P., Irvine, J.R., 1995. Sackungen at the Aspen high-lands ski area, Pitkin County, Colorado. Environ. Eng. Geosci. 1, 277-290.

Miccadei, E, Barberi, R, Cavinato, G.P., 1998. La geologia quaternaria della conca di Sulmona (Abruzzo, Italia centrale). Geologica Romana 34, 59–86.

Miccadei, E., Paron, P., Piacentini, T., 2004. The SW escarpment of Montagna del Morrone (Abruzzi, central Italy): geomorphology of a fault-generated mountain front. Geogr. Fis. Din. Quat. 27, 55-87.

Moro, M., Saroli, M., Salvi, S., Stramondo, S., Doumaz, F., 2007. The relationship between seismic deformation and deep-seated gravitational movements during the 1997 Umbria–Marche (Central Italy) earthquakes. Geomorphology 89, 297-307.

Moro, M., Saroli, M., Tolomei, C., Salvi, S., 2009. Insights on the kinematics of deep seated gravitational slope deformations along the 1915 Avezzano earthquake fault (central Italy), from time-series DInSAR. Geomorphology 112, 261-276.

Moro, M., Chini, M., Saroli, M., Atzori, S., Stramondo, S., Salvi, S., 2011. Analysis of large, seismically induced, gravitational deformations imaged by high resolution COSMO-SkyMed SAR. Geology 39, 527-530.

Moro, M., Saroli, M., Gori, S., Falcucci, E., Galadini, F., Messina, P., 2012. The interaction between active normal faulting and large scale gravitational mass movements revealed by paleoseismological techniques: a case study from central Italy. Geomorphology 151/152, 164-174.

Onida, M., 2001. Deformazioni gravitative profonde: stato delle conoscenze e progresso delle ricerche in Italia. In: Pasquarè, G. (Ed.), Tettonica Recente e Instabilità di Versante nelle Alpi Centrali. CNR, Istituto per la Dinamica dei Processi Ambientali, Milano, Italy, pp. 35-74.

Papanikolaou, I. D., Roberts, G.P., Michetti, A.M., 2005. Fault scarps and deformation rates in Lazio–Abruzzo, Central Italy: comparison between geological fault slip-rate and GPS data. Tectonophysics 408, 147-176.

Pasuto, A., Soldati, M., 1996. Rock spreading. In: Dikau, R., Brunsden, D., Schrott, L., Ibsen M.-L. (Eds.), Landslide Recognition: Identification, Movement and Causes. John Wiley & Sons Ltd., Chichester, pp. 122-136.

Patacca, E., Scandone, P., 1989. Post-Tortonian mountain building in the Apennines. The role of passive sinking of a relic lithosphere slab. In: Boriani, A., Bonafede, M., Piccardo, G.B., Vai, G.B. (Eds.), The Lithosphere in Italy. Advances in Earth Science Research, Atti Convegni Lincei80, 157-176.

Pizzi, A., Pugliese, G., 2004. InSAR-DEM analyses integrated with geologic field methods for the study of long-term seismogenic fault behavior: Applications in the axial zone of the central Apennines (Italy). J. Seismol. 8, 313-329.

Roberts, G.P., Michetti, A.M., 2004. Spatial and temporal variations in growth rates along active normal fault systems: an example from the Lazio–Abruzzo Apennines, central Italy. J. Struct. Geol. 26, 339-376.

Rovida, A., Camassi, R., Gasperini, P., Stucchi, M. (Eds.) 2011. CPTI11, la Versione 2011 del Catalogo Parametrico dei Terremoti Italiani. Milano, Bologna, http://emidius.mi.ingv.it/CPTI.

Schlagenhauf, A., Manighetti, I., Benedetti, L., Gaudemer, Y., Finkel, R., Malavieille, J., Pou, K., 2011. Earthquake supercycles in central Italy, inferred from ^{36}Cl exposure dating. Earth Planet. Sci. Lett. 307, 487-500.

Soldati, M., 2004. Deep-seated gravitational slope deformation. In: Goudie, A.S. (Ed.), Encyclopedia of Geomorphology. Routledge, London, pp. 226-228.

Vannoli, P., Burrato, P., Fracassi, U., Valensise, G., 2012. A fresh look at the seismotectonics of the Abruzzi (central Apennines) following the 6 April 2009 L'Aquila earthquake (Mw 6.3). Boll. Soc. Geol. It. (Int. J. Geosci.) 131 (3), 309-329.

Varnes, D.J., 1978. Slope movements types and processes. In: Schuster R.L., Krizek R.J. (Eds.), Landslides: Analysis and Control. Special Report 176, Transportation Research Board, Washington, D.C., pp. 11-35.

Vezzani, L., F., Ghisetti, 1998. Carta Geologica dell'Abruzzo, scala 1:100.000, S.El.Ca., Firenze.

Vittori, E, Cavinato, G.P., Miccade,i E., 1995. Active faulting along the northeastern edge of the Sulmona basin, central Apennines, Italy. In: Serva L, Slemmons D.B. (Eds.) Perspective in Paleoseismology. Special Publication-Association of Engineering Geologists, vol. 6, pp. 115-126.

Wells, D.L., Coppersmith, K.J., 1994. New empirical relationships among magnitude, rupture length, rupture width, rupture area, and surface displacement. B. Seismol. Soc. Am. 84, 974-1002.

Zischinsky, U., 1969. ÜÜber Sackungen. Rock- Mech. 1, 30-52.

Figure captions

Fig. 1. Seismotectonic framework of the central Apennines with main active normal fault systems (modified from Galadini and Galli, 2000; Falcucci et al., 2011 and references therein) and the epicentres of the largest earthquakes that struck the region in the past millennium (Rovida et al., 2011). Faults: MVF – Mt. Vettore; NF – Norcia; LM – Laga Mountains.; UAVF – Upper Aterno Valley; ACIF – Assergi-Campo Imperatore; CF-OPF – Campo Felice-Ovindoli-Pezza; MAVF-SVF – Middle Aterno Valley-Subequana Valley; MMF – Mt. Morrone; FF – Fucino; MPF – Maiella-Porrara; ACF – Aremogna-Cinquemiglia; USVF – Upper Sangro Valley.

Fig. 2. Perspective shaded relief images showing the Sulmona Plain and the south-western flank of Mt. Morrone. The trace of the active fault segments are marked by black lines in (a); the main *sackung*-related troughs are reported in (b) with white dashed lines.

Fig. 3. Digital elevation model of the Sulmona Plain and of Mt. Morrone. Contour interval is 25 m.

Surveyed DGSD features and the main normal fault segments are reported. Inset is the geomorphic-structural profile. 1. Gravitational trough. 2. Active normal fault, as observed (a) and presumed (b). 3. Inactive thrust front. 4. Excavation site. 5. Location of the geomorphic-structural profile.

Fig. 4. Evidence of the fault scarplet north-west of Roccacasale. (a) Digital elevation model of the area of Roccacasale. 1. Le Pietre-Pianezza rock slide scarp. 2. Trace of the “Colle della Paglia” gravitational trough. 3. Mt. Morrone western fault branch. 4. Inferred abandoned fault scarps. White circle: outcrop of tectonically displaced slope debris showen in (c). (b) Fault plane seen at the base of the scarplet, north of Roccacasale, in contact with carbonate rocks at the hanging wall and footwall. (c) Slope-derived deposits (white arrows) displaced and dragged along the fault plane, north of Roccacasale.

Fig. 5. Panoramic view of the Roccacasale area. (a, b) and frontal view of the Le Pietre-Pianezza rock slide. Triangles show the fault scarp probably displaced by DGSD movements; and white arrows show the fault scarplet representing the current fault segment. (c) and (d) Three-dimensional lateral view and simplified geological cross-section of the Le Pietre-Pianezza rock slide. 1. Carbonate bedrock. 2. Slope-derived deposits. 3. Alluvial sediments. 4. Present thalweg of the Sagittario River. 5. Fault segment. 6. Rock slide scarp. 7. Displaced fault plane and scarp. 8. Gravitational trough. 9. Gravitational deformation/sliding zone. 10. Gravitational sliding plane.

Fig. 6. The Pacentro paleo-landslide. (a and b) Digital elevation model (plan view) of the Pacentro area, with the Pacentro paleo-landslide accumulation and Middle Pleistocene alluvial fan deposits. White dashed line – contact between the Middle Pleistocene alluvial fan and the paleo-landslide accumulation in the Pacentro area (inset). (c) Three-dimensional view of the Pacentro area, showing the accumulation of the Pacentro paleo-landslide deposits. d) Close-up image of the Mt. Morrone double-crested ridge and of the bulged sector at the base of the slope. e) Photograph of the

Pacentro paleo-landslide scarp (shown by black triangles). 1. Fault splay, as observed (solid line) and presumed (dashed line). 2. Presumed landslide scarp. 3. Landslide accumulation. 4. Gravitational trough.

Fig. 7. The Mt. Orsa gravitational trough and excavation sites. (a) Digital elevation model. Traces of the gravitational trough and other *sackung*-related troughs are marked (white lines). (b) Three-dimensional frontal view of the Mt. Orsa area, where Early Pleistocene breccias are observed (see inset). (c) Excavation site along the Mt. Orsa gravitational trough. Inset shows the locations of the western and eastern trenches. (d) Early Pleistocene breccias cropping out along both flanks of the trough (white line). The breccias along the western flank are clearly deformed and tilted by the opening of the gravitational trough (see inset). Black dashed line shows the attitude of the deposits..

Fig. 8. Views (a, b) and illustrations (c, d) of the northern walls of the Mt. Orsa western and eastern trenches, respectively. Stratigraphic units are described in the text. (e) Scarp (white dashed line) of a small rock slide within the Mt. Orsa gravitational trough. (f) View of the northern wall of the western trench that exposes the sliding plane of the rock slide (white line). Excavation grid is 1×1 m.

Fig. 9. The Colle della Paglia gravitational trough and excavation sites. (a) Digital elevation model. White line – traces of the Colle della Paglia and of other gravitational troughs. Black line – the Mt. Morrone western fault segment. (b) Three-dimensional frontal view of the Colle della Paglia gravitational trough. The excavation site for paleoseismological investigations is indicated. (c) Panoramic view of the excavation site. Two trenches were excavated across the downhill-facing and uphill-facing scarps of the trough.

Fig. 10. Views (a, b) and illustrations (c, d) of the northern walls of the Colle della Paglia west and east excavations. Stratigraphic units are described in the text. (e, f) Shear planes (white arrows) detected along the northern and southern walls of the west excavation, respectively. Excavation grid is 1×1 m.

Fig. 11. Schematic representation of the structural and geomorphic evolution of the Mt. Morrone south-western slope during the Quaternary. 1. Inactive thrust plane. 2. Active normal fault plane and related deformation zone. 3. Gravitational trough. 4. Gravitational sliding zone/plane. 5. Continental sedimentary sequences. 6. Mesozoic–Cenozoic limestone. 7. Miocene–Pliocene flysch and hemipelagic clays and marls.

Table 1. Results of radiocarbon dating.

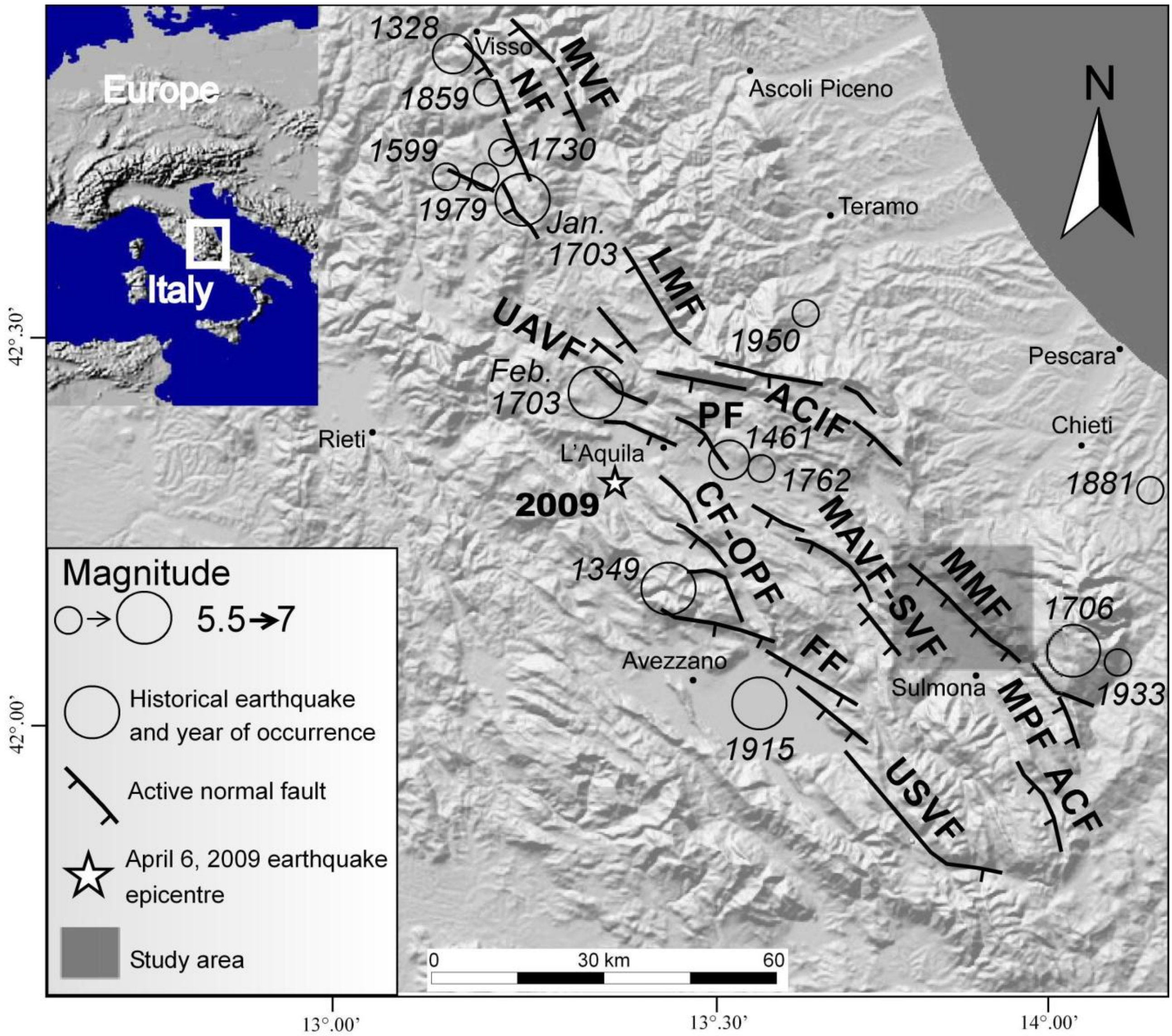
Europe
Italy
N
1328
Visso
MVF
1859
NF
Ascoli Piceno
1599
1730
1979
Jan.
1703
Teramo
LMF
UAVF
1950
Pescara
Feb.
1703
PF
ACIF
Rieti
L'Aquila
1461
Chieti
1762
1881
2009
CF-OPF
MAVF-SVF
MMF
1349
1706
FF
Avezzano
Sulmona
MPF
1933
1915
ACF
USVF
Magnitude
5.5→7
Historical earthquake and year of occurrence
Active normal fault
April 6, 2009 earthquake epicentre
Study area
0
30 km
60
42°.30'
42°.00'
13°.00'
13°.30'
14°.00'

Figure 1

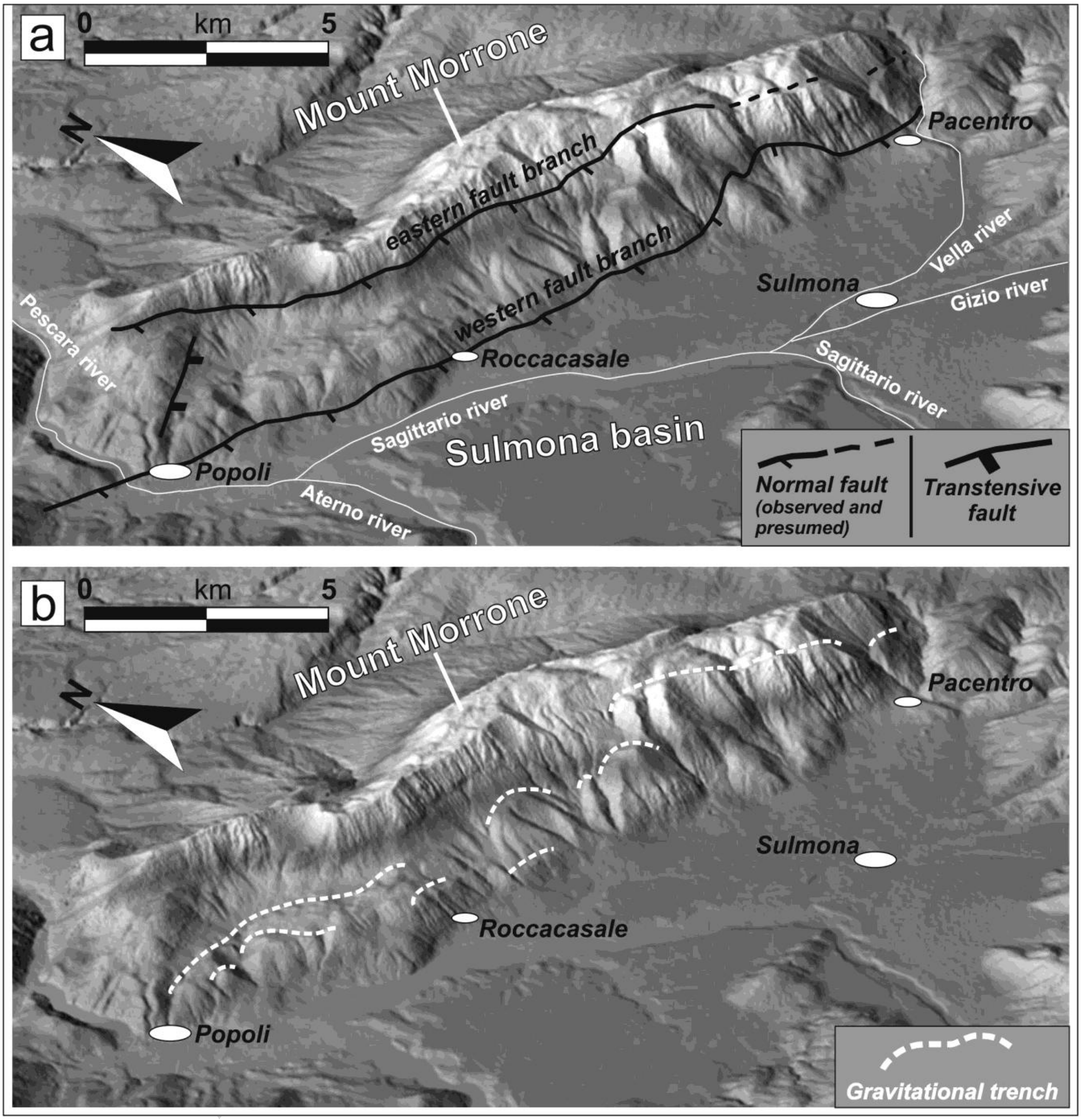
a
0
km
5
Mount Morrone
eastern fault branch
western fault branch
Pacentro
Vella river
Sulmona
Gizio river
Pescara river
Roccacasale
Sagittario river
Sagittario river
Sulmona basin
Popoli
Aterno river
Normal fault
(observed and
presumed)
Transtensive
fault
b
0
km
5
Mount Morrone
Pacentro
Sulmona
Roccacasale
Popoli
Gravitational trench

Figure 2

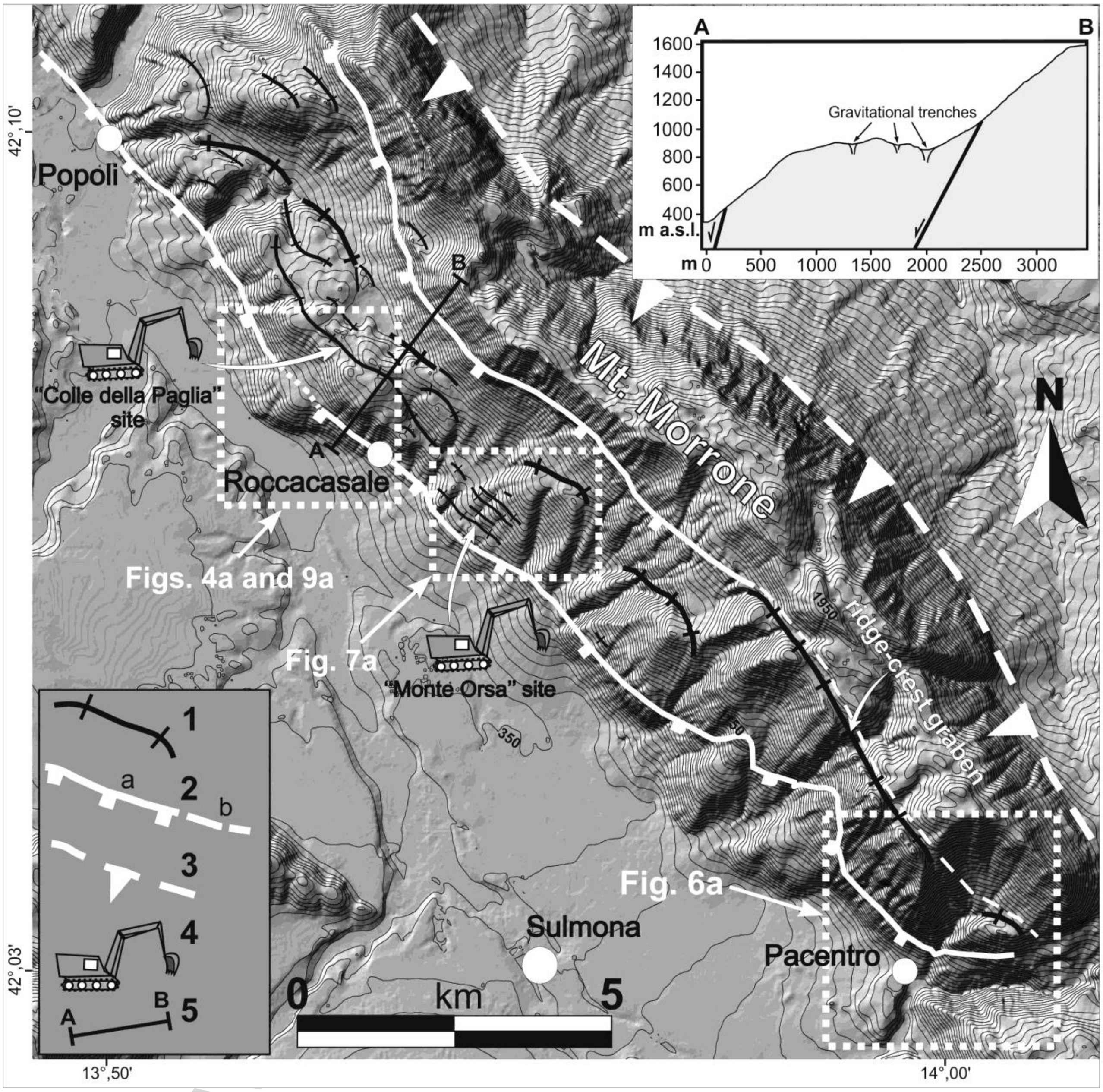
A
B
1600
1400
1200
1000
800
600
400
m a.s.l.
m 0
500
1000
1500
2000
2500
3000
Gravitational trenches
42°,10'
42°,03'
13°,50'
14°,00'
Popoli
"Colle della Paglia" site
Roccacasale
Figs. 4a and 9a
Fig. 7a
"Monte Orsa" site
Mt. Morrone
ridge-crest graben
1950
350
N
Fig. 6a
Sulmona
Pacentro
0
km
5
1
2
a
b
3
4
5

Figure 3

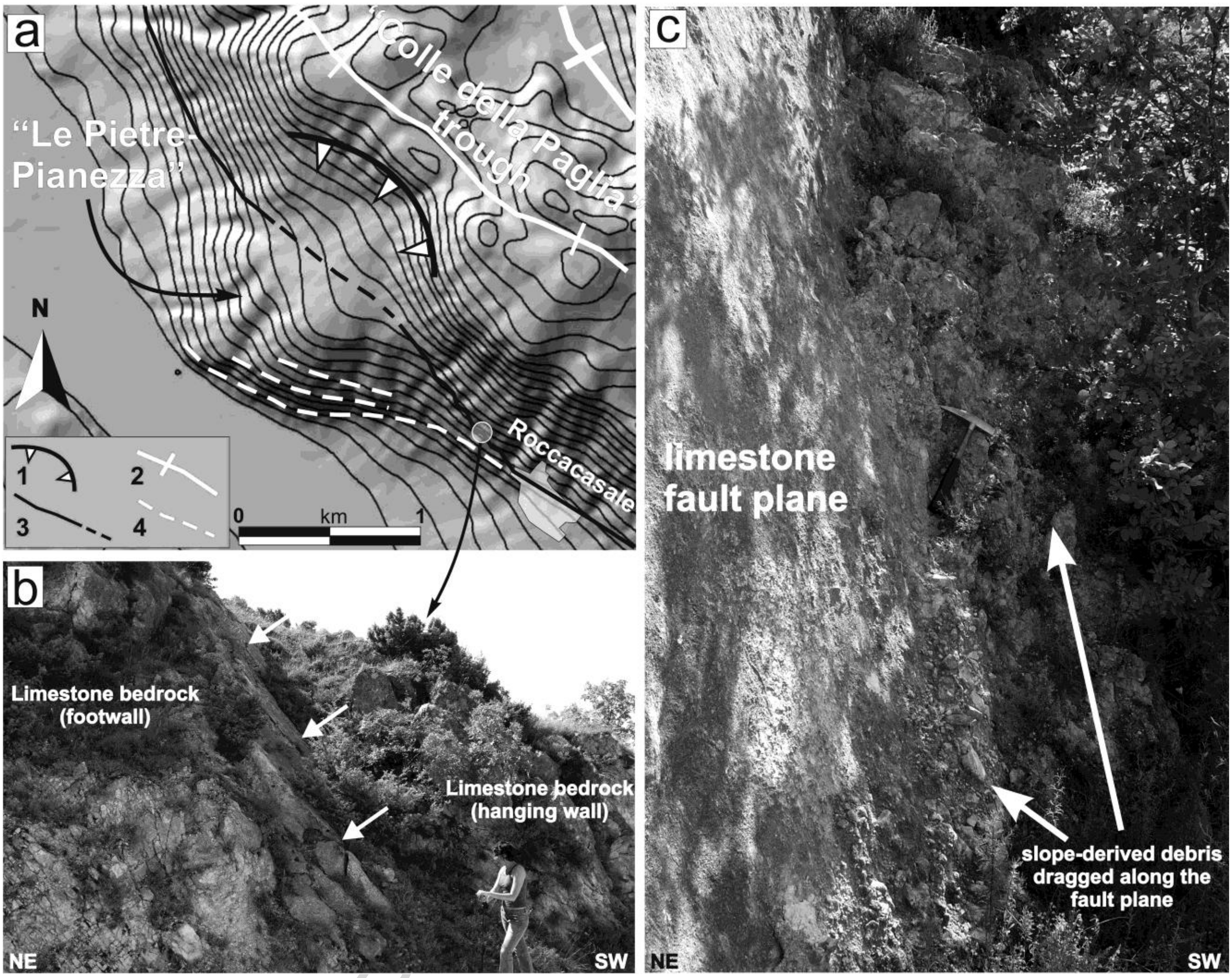
a
"Le Pietre-Pianezza"
"Colle della Paglia" trough
N
Roccacasale
1
2
3
4
0
km
1
b
Limestone bedrock (footwall)
Limestone bedrock (hanging wall)
NE
SW
c
limestone fault plane
slope-derived debris dragged along the fault plane
NE
SW

Figure 4

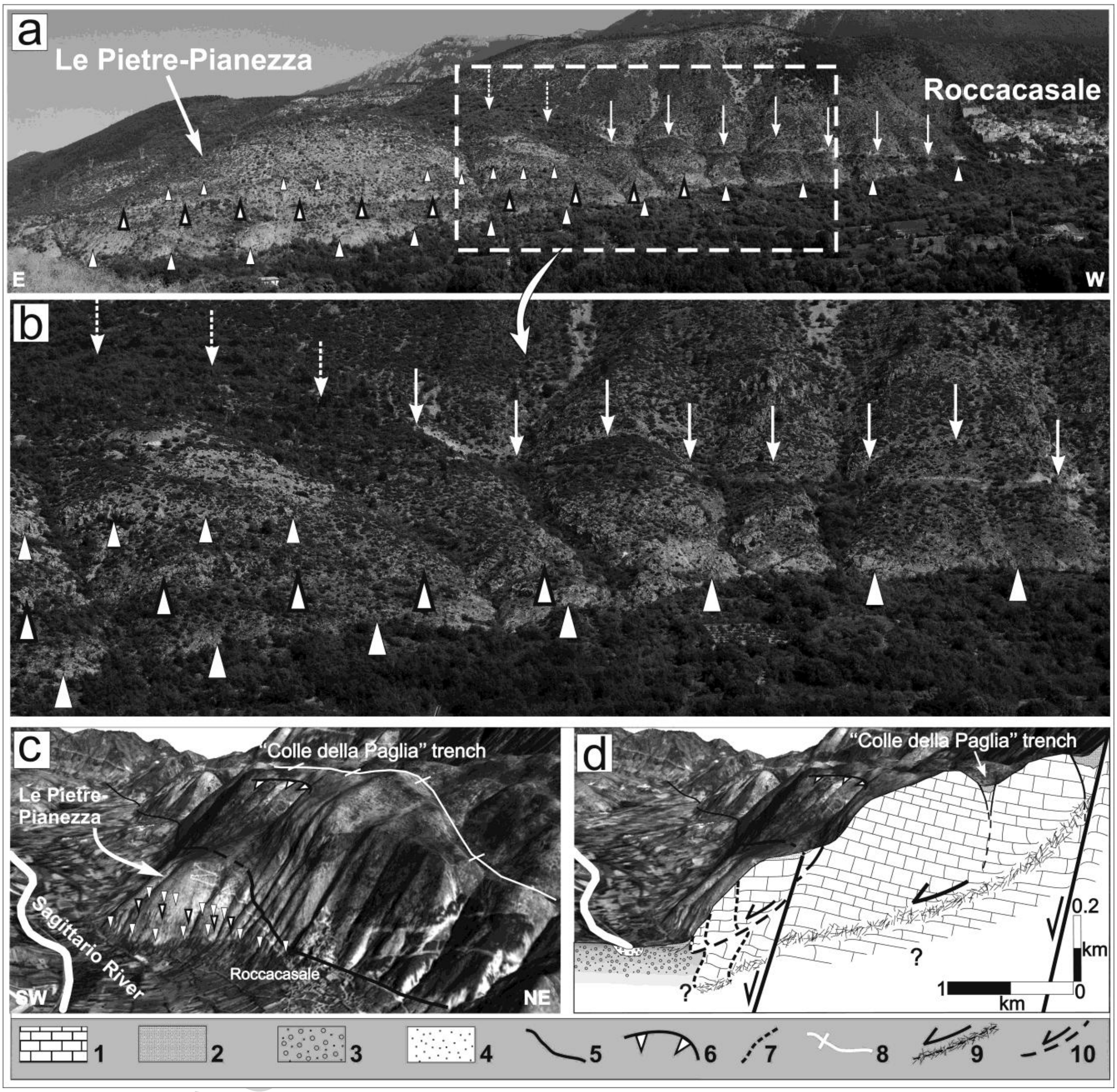
a
Le Pietre-Pianezza
Roccacasale
E
W
b
c
"Colle della Paglia" trench
Le Pietre-Pianezza
Sagittario River
Roccacasale
SW
NE
d
"Colle della Paglia" trench
?
?
?
0.2
km
0
1
km
1
2
3
4
5
6
7
8
9
10

Figure 5

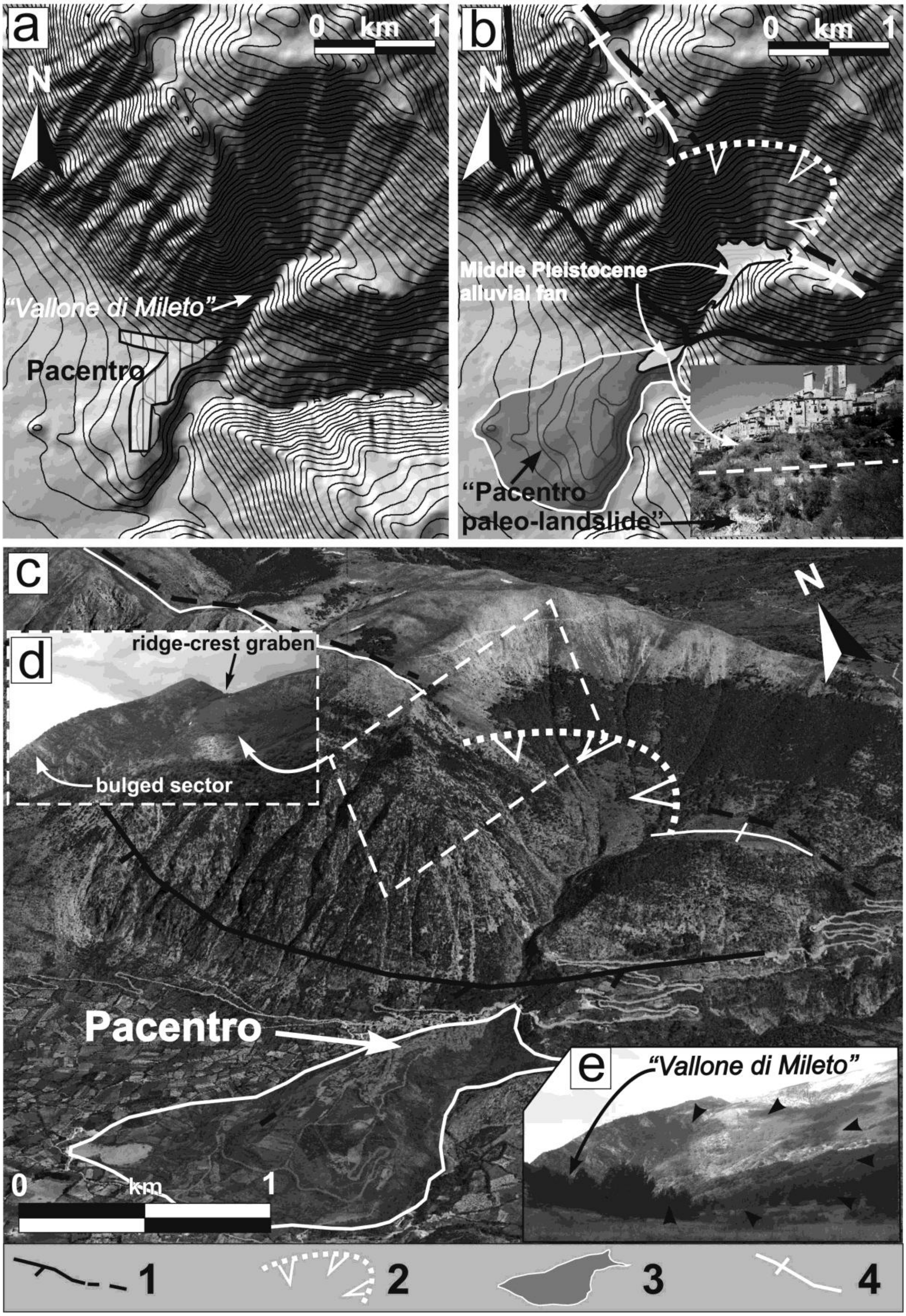
a
0 km 1
N
"Vallone di Mileto"
Pacentro
b
0 km 1
N
Middle Pleistocene alluvial fan
"Pacentro paleo-landslide"
c
N
d
ridge-crest graben
bulged sector
Pacentro
e
"Vallone di Mileto"
0 km 1
1
2
3
4

Figure 6

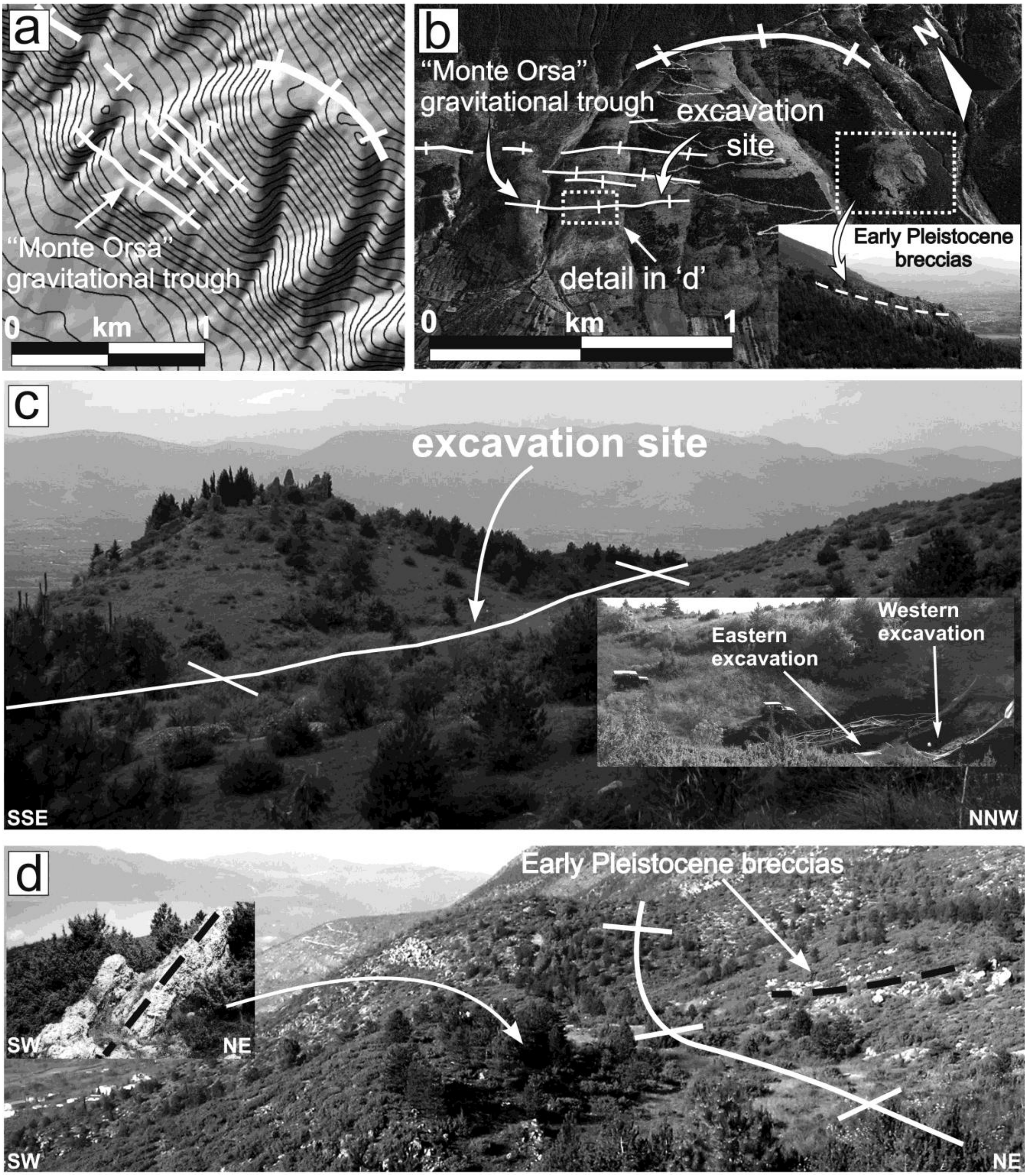

a
"Monte Orsa"
gravitational trough
0
km
1
b
"Monte Orsa"
gravitational trough
excavation
site
N
Early Pleistocene
breccias
detail in 'd'
0
km
1
c
excavation site
Eastern
excavation
Western
excavation
SSE
NNW
d
Early Pleistocene breccias
SW
NE
SW
NE

Figure 7

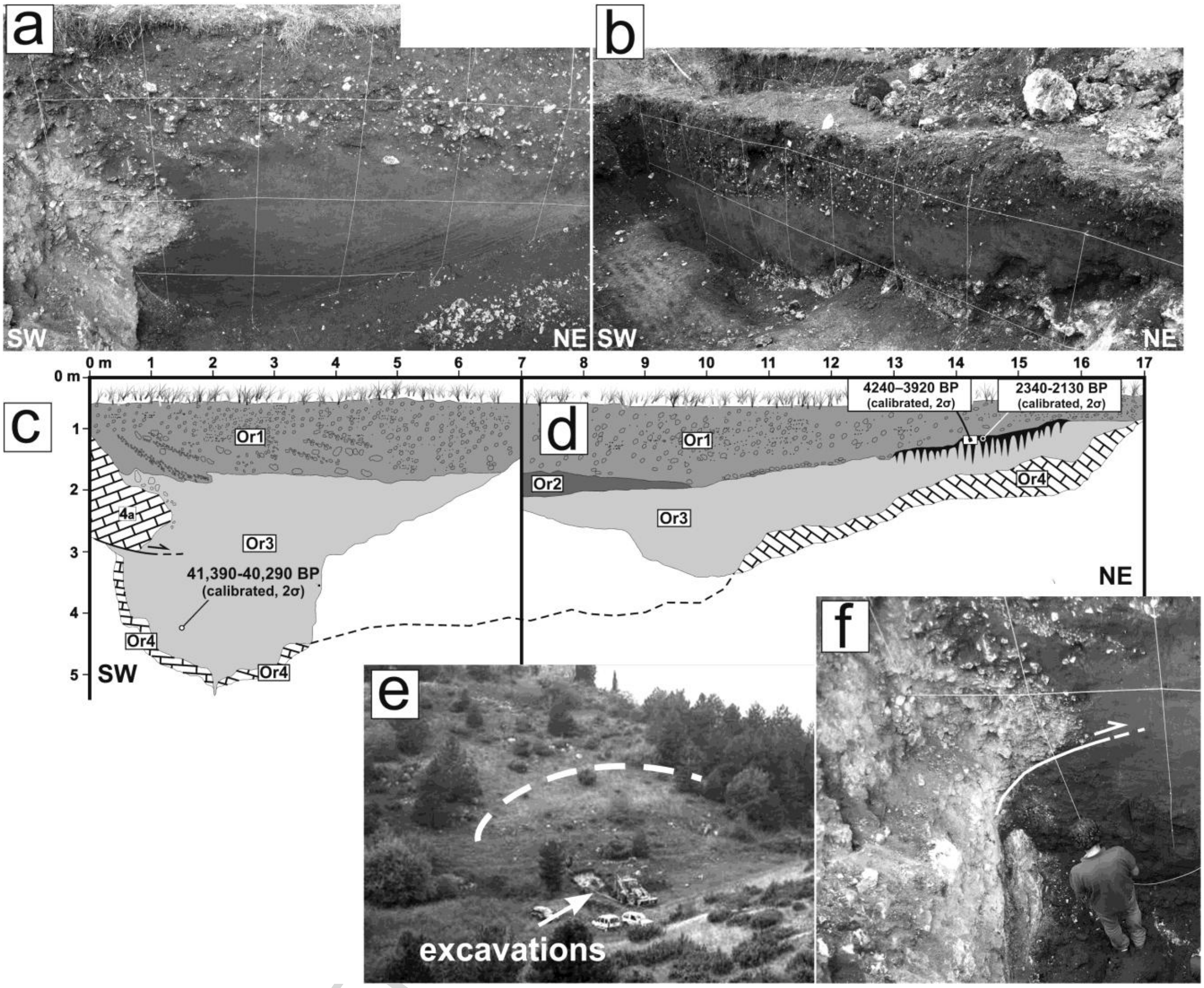
a
b
SW
NE
SW
NE
0 m
1
2
3
4
5
6
7
8
9
10
11
12
13
14
15
16
17
c
d
Or1
Or1
Or2
Or3
Or3
Or4
Or4
Or4
4a
4240–3920 BP
(calibrated, 2σ)
2340-2130 BP
(calibrated, 2σ)
41,390-40,290 BP
(calibrated, 2σ)
SW
NE
e
f
excavations

Figure 8

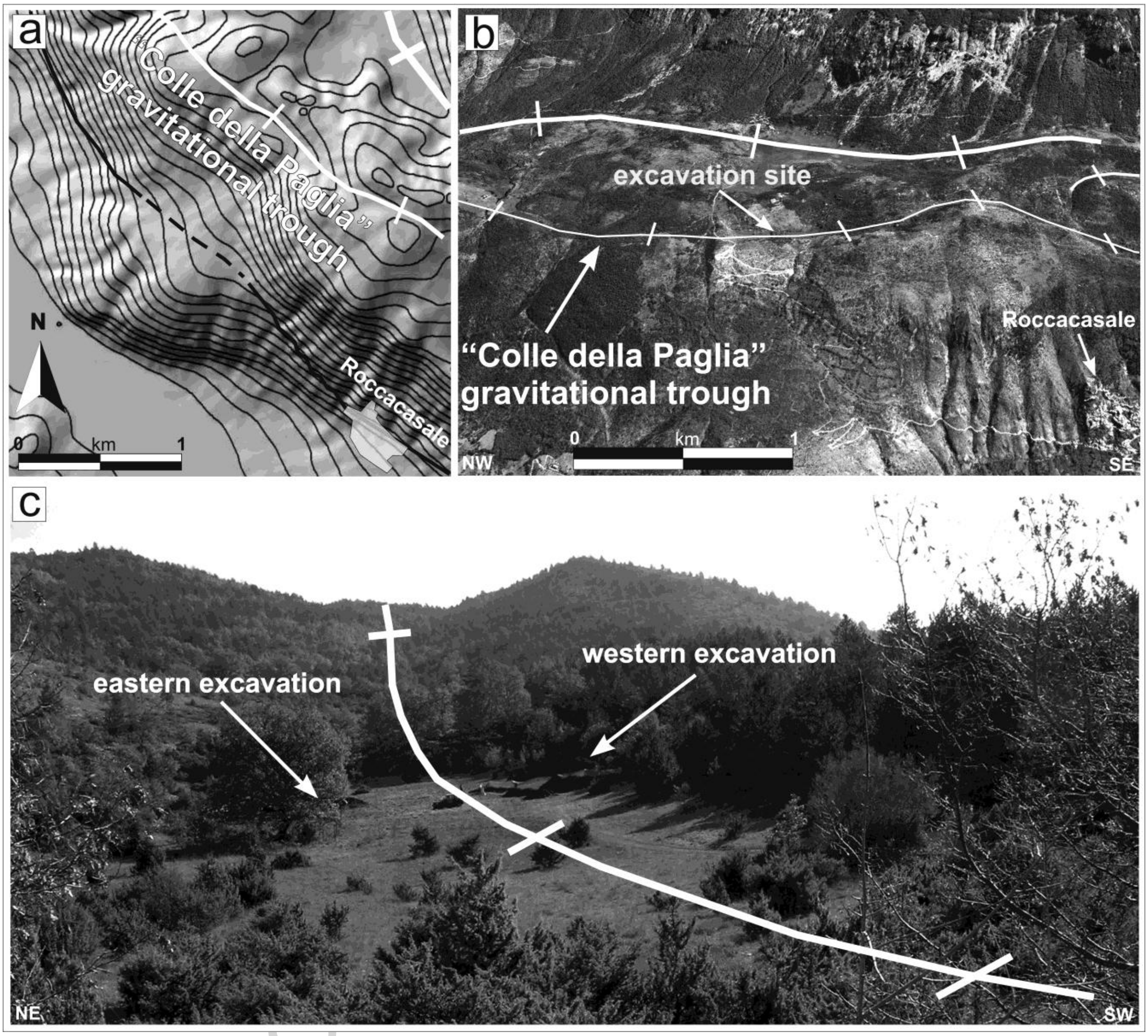
a
"Colle della Paglia" gravitational trough
N
Roccacasale
0 km 1
b
excavation site
"Colle della Paglia" gravitational trough
Roccacasale
NW
0 km 1
SE
c
eastern excavation
western excavation
NE
SW

Figure 9

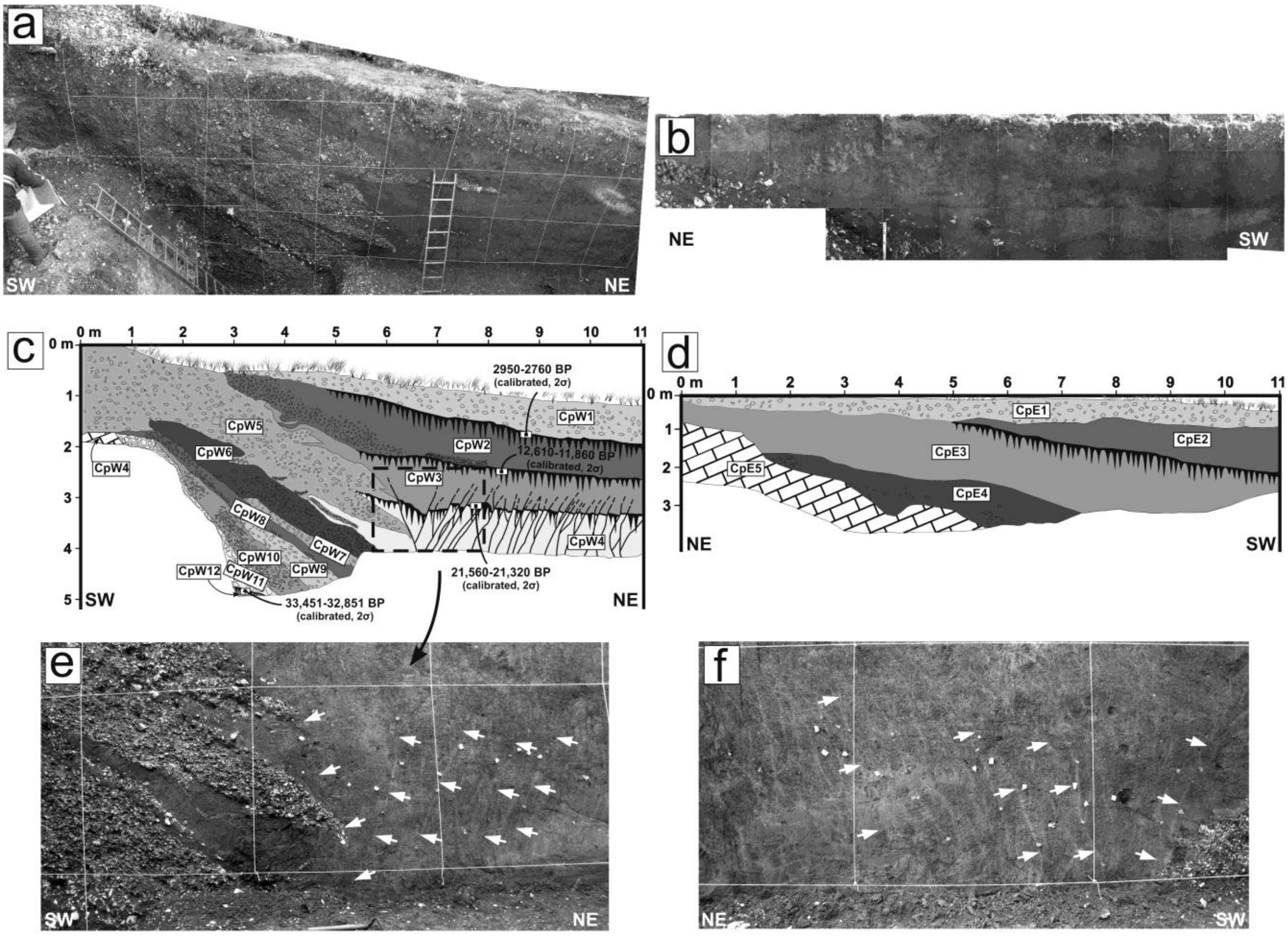

a
SW
NE
b
NE
SW
c
0 m
1
2
3
4
5
6
7
8
9
10
11
2950-2760 BP
(calibrated, 2σ)
CpW1
CpW2
12,610-11,860 BP
(calibrated, 2σ)
CpW3
CpW4
CpW5
CpW6
CpW7
CpW8
CpW9
CpW10
CpW11
CpW12
21,560-21,320 BP
(calibrated, 2σ)
33,451-32,851 BP
(calibrated, 2σ)
SW
NE
d
CpE1
CpE2
CpE3
CpE4
CpE5
NE
SW
e
SW
NE
f
NE
SW

Figure 10

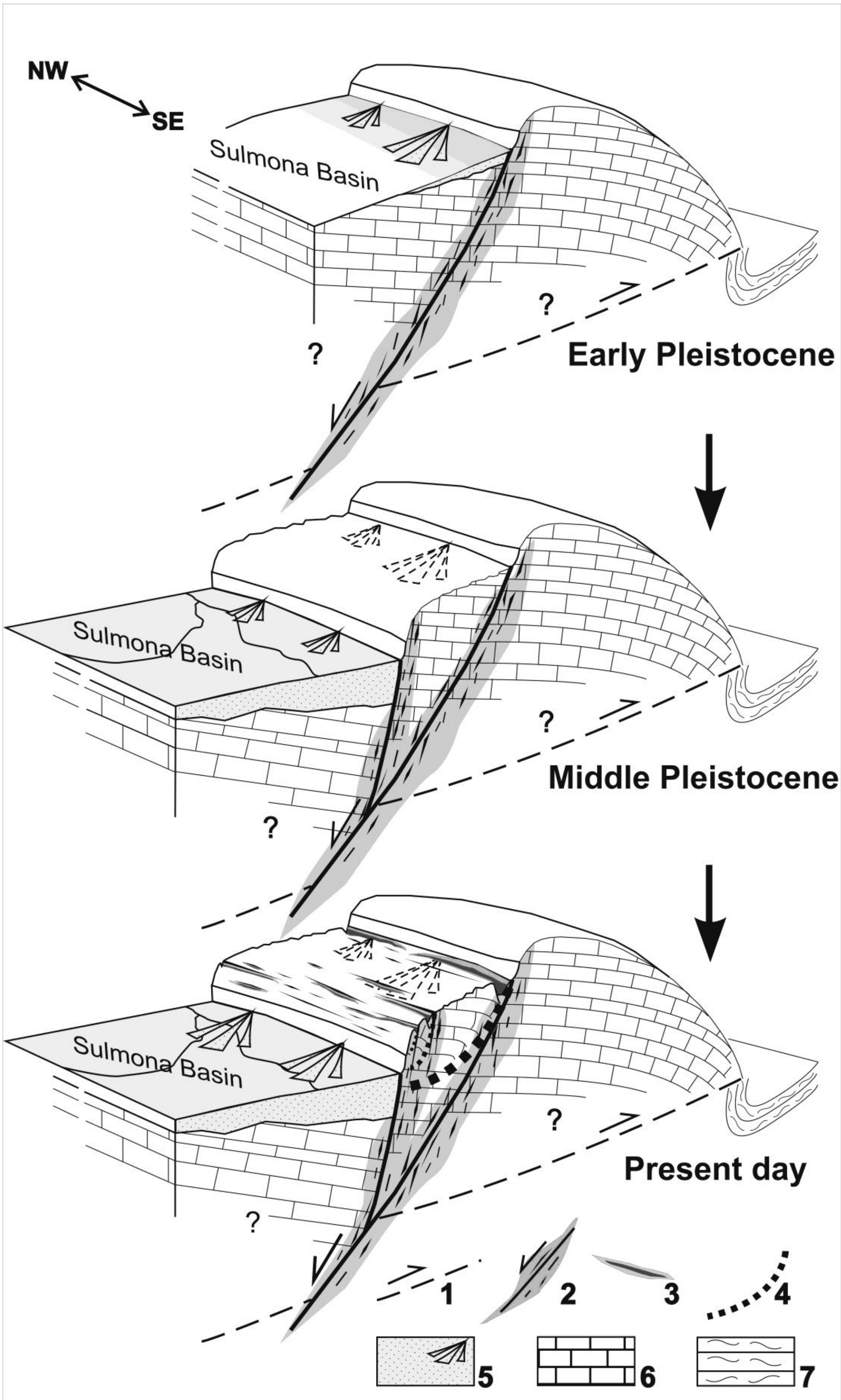
NW
SE
Sulmona Basin
?
?
Early Pleistocene
Sulmona Basin
?
?
Middle Pleistocene
Sulmona Basin
?
?
Present day
1
2
3
4
5
6
7

Figure 11

Table 1

excavation	Unit	dated material	radiocarbon age (calibrated, 2σ)
Monte Orsa western	Or3	charcoal	2235±105BP
		paleosol	4080±160BP
		charcoal	40840±550BP
Colle della Paglia western	CpW2	paleosol	2855±89BP
	CpW3	paleosol	12235±375BP
	CpW4	paleosol	21440±120BP
	CpW12	paleosol	33151±300BP

ACCEPTED MANUSCRIPT